Mechanical Performance of Timber Connection made by Wood Welding Technique

by

Xiaoyu Wang

Bachelor of Science in Engineering (Material Science and Engineering), Nanjing

Forestry University, P. R. China, 2021

A Report Submitted in Partial Fulfillment
of the Requirements for the Degree of

Master of Forestry Engineering

in the Graduate Academic Unit of Forestry and Environmental Management

Supervisor: Meng Gong, PhD, Forestry and Environmental Management

Examining Board: Huining Xiao, PhD, Chemical Engineering
Alireza Kaboorani, PhD, Forestry and Environmental Management

This report is accepted by the
Dean of Graduate Studies

THE UNIVERSITY OF NEW BRUNSWICK

August, 2022

ABSTRACT

A new type of timber connection is developed using the wood friction welding technique, which is a non-adhesive gluing process. During this process, heat is needed to melt the wood material in the course of pressing one wood piece to another via linear vibration or rotation. The objective of this study was to investigate the mechanical performance of timber connections made via the rotation welding. The spruce-pine-fir (S-P-F) lumber was used to fabricate the members, and the sugar maple (*Acer saccharum*) was used to make the dowels with a diameter of 19mm (3/4"). The bolts were used to make the timber connections as well as for comparison purpose. Two loading directions (parallel (PA) and perpendicular (PE)) and three connection types (push-in dowel (P), welding dowel (W), and bolted (B)), were considered in the design of experiment. There were two (2) groups of three (3) sets each. Each set had six (6) replicates, making a total of 36 specimens. Each joint specimen was performed on a universal mechanical testing machine. It was found that (1) The peak load and initial stiffness of set PA-B were 33kN and 5kN/mm, which were about 135% larger than and 45% less than set PA-W. The peak load and initial stiffness of set PA-P were 14% and 50% larger than that of set PA-W. (2) The yield loads for sets PA-P and PA-W were almost the same, being 13kN, which were about 150% lower than that of set PA-B. (3) The ductility and energy accumulated of set PA-B were about 30% less than and 140% larger than set PA-W. (4) The average peak load and initial stiffness of group PA were about 25% and 27% greater than those of group PE.(5) Johansen Theory was found to be conservative in derivation of engineering design values of wood dowelled and metal bolted joints. (6) The failure of wood doweled joint specimens was the fracture

of the dowels, and the failure of bolted joint specimens was the crushing of member wood. (7) The mechanical properties of welded joints were similar to those of push-in joints. (8) The welding process did not generate cracks, minimizing stress concentrations, in wood members, in comparison to push-in process. It has great potential in fabrication of dowel-laminated wood products and repair/reinforcement of laminated beams. As for the future work, application of welding techniques should be explored during the manufacturing and construction of timber products and buildings, such as reinforcing glued laminated wood with notches.

Key words: wood welding, timber joints, peak load, initial stiffness, yield load, ductility, energy dissipation, European Yield Model.

ACKNOWLEDGEMENTS

This report is the end of a long and arduous journey that I have only been able to make as a result of the dedicated support I have received from so many people along the way. First, I would like to thank the 3+1+1 Program between the University of New Brunswick (UNB) and Nanjing Forestry University (China), and the New Brunswick Innovation Research Chair Initiative Program, New Brunswick Innovation Foundation, Canada.

I would like to express my deepest and sincerest gratitude to my supervisor, Dr. Meng Gong, for his continued and invaluable guidance throughout my research. It is a great honor that I was given the opportunity to work under his supervision. I would like to thank him for his patience, support, empathy, and great sense of humor. I also want to thank the seniors at the Wood Science and Technology Center, the University of New Brunswick, for their advice. I also appreciated the support from Mr. Greg McCarthy for helping me to make the specimens and conduct the tests.

I would like to thank my friends for their encouragement and support. We support each other in our study and life, which is a precious experience for me. I am very grateful to my parents for their patience, love and care in my education and life journey. I offer my sincere wishes for everything pleasant for you.

Table of Contents

List of Tables

List of Figures

List of symbols, Nomenclature or Abbreviations

American Society for Testing and Material	ASTM
Cross Laminated Timber	CLT
Engineering Wood Product	EWP
Polyvinyl acetate	PVAc
Spruce-Pine-Fir	S-P-F
European Yield Model	EYM
Glass transition temperature	T_g
Scanning Electron Microscopy	SEM
Thermogravimetric	TG
Stiffness	K
Relative Humidity	RH
Moisture Content	MC
Linearly Variable Differential Transformer	LVDT
Parallel	PA
Perpendicular	PE
Bolted	B
Push-in	P
Welded	W

1 Introduction

1.1 Background

1.1.1 Wood and engineered wood products

Wood is a renewable, recyclable and sustainable natural resource. Historically, it has been used to make interior furniture, doors and windows, and exterior structures due to its light weight and suitable stiffness and strength. Compared to steel and concrete, which require a lot of energy in the process of making these materials, wood building materials are an environmentally friendly and economical choice.

Nowadays, the use of wood as a modern building material for structures such as high-rise buildings and large houses has become a demand. To meet these needs, the technologies of processing wood continue to advance, and more engineered wood products (EWPs) have been invented and used in construction.

An EWP is a product fabricated with wood materials and adhesives and/or fasteners (such as nails) targeted mainly for structural applications. It offers many advantages over traditional solid timber products: (1) EWPs can reach a size that is not constrained by the tree dimension; (2) EWPs accommodate a wide spectrum of species and sizes of trees, allowing more efficient utilization of raw wood materials in the form of fibers, strands, veneers, and lumber; (3) EWPs can be more easily adopted to market requirements than solid wood due to their designability (Gong, 2021). Figure 1-1 illustrates various EWPs.

Figure 1-1 Engineered wood products (Source: Gong, 2022)

1.1.2 Wood connection

The strength and stability of a structure heavily depend on the fastenings that hold its parts together. One prime advantage of wood as a structural material is the ease with which wood structural parts can be joined together with a wide variety of fastenings such as nails, spikes, screws, bolts, lag screws, drift pins, staples, and metal connectors of various types. For wood connectors, they are usually divided into small-diameter (nails, spikes, and wood screws) and large diameter dowel-type fasteners (bolts, lag screws, and drift pins) (Wood Handbook, 1974). Figure 1-2 shows the major dowel-type fasteners.

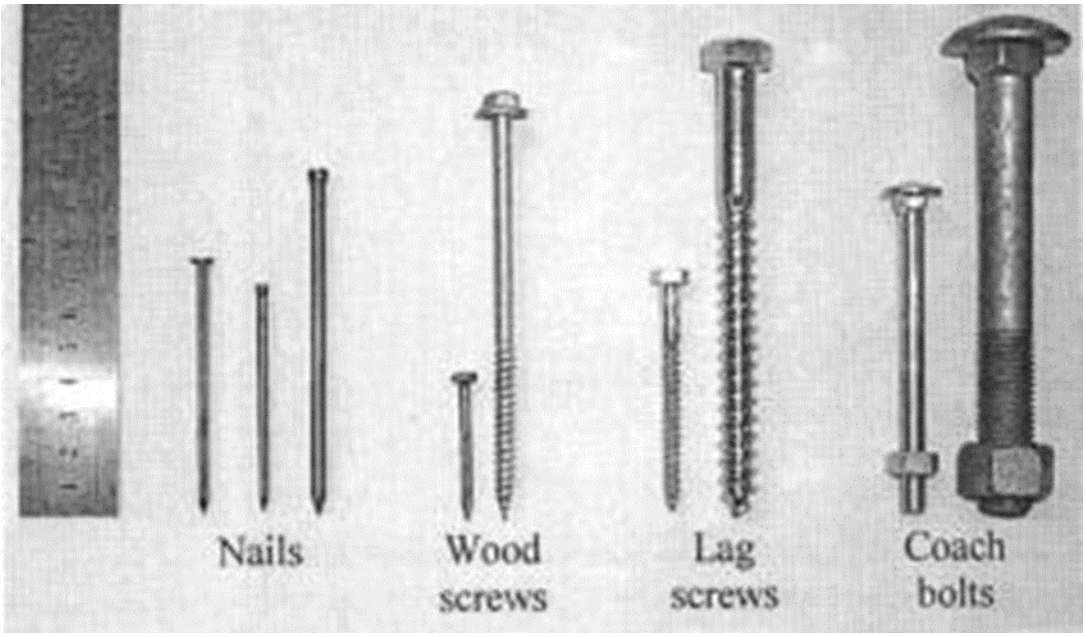

Figure 1-2 Major dowel-type fastener joints

(Source: Smith & Foliente, 1989).

1.1.3 Wood welding technology

Friction welding is a non-adhesive gluing process. During this process, heat is needed to melt the wood material in the course of pressing one wood piece to another via linear vibration or rotation. The welding principle is that the hemicellulose and lignin are softened and fused by the relative movement of a specimen to form an intersecting network structure in the interface layer. After cooling and curing, the bonding is realized.

Wood welding has been used in the production of timber construction such as wood buildings. For the linear welding, it was investigated for use in the production of cross laminated timber (CLT), a wood structure product, as an alternative to polyurethane bonded wood components (Hahn, 2013). For the rotational welding, it can be applied by reserving holes in a wood structure specimen that need to be connected, and then connecting them together through a rotational dowel. This function is similar to that of nails. Bocuqet and Pizzi (2012) designed and fabricated a 4m² floor by rotational wood welding, and found that both static and dynamic load capacities could meet the requirements stipulated in Eurocode5 “Design of timber structures. Part 1-1: General. Common rules and rules for buildings, Final Draft (CEN, 2013)”.

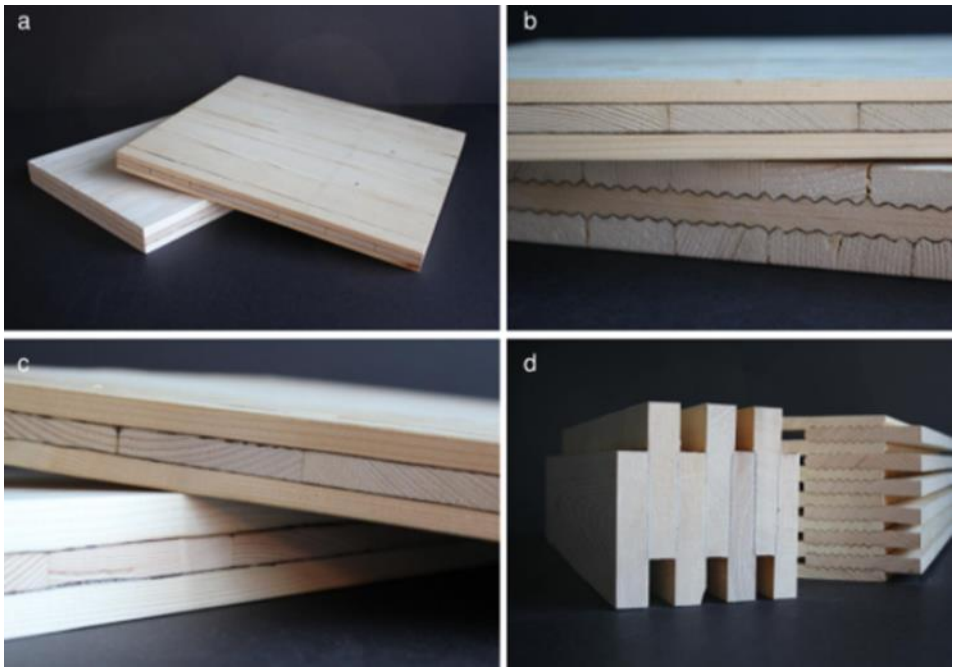

Figure 1-3 First small scale prototype of potential industrial applications of the friction welding technology in production of CLT (Source: Hahn, 2013).

Figure 1-4 Configuration of welded dowels during floor construction

(Source: Bocuqet & Pizzi, 2012).

Meanwhile, wood rotational welding can also apply in the manufacturing panel produced through this technique, for example, blockboard. A blockboard is an assembly of wood pieces bonded together, often using PVAc adhesive. The high-speed dowel rotation wood welding can replace the traditional adhesive (Segovia & Zhou, 2013). Wood welding could scale up the technique to create large structural elements, such as beams and floor assemblies (Bellevlle & Segovia, 2010).

Gluing is a valid and extensively used alternative to paneling in the furniture industry and timber construction such as wood buildings. However, adhesives, which are generally produced by the petrochemical industry, require long curing times and multiple handling, which limits the production flow and flexibility required. Air pollution and harmful working conditions are also major problems (Belleville & Pizzi, 2012). Wood welding can quickly produce very strong joints and does not require any adhesive. At the same time, rotational wood welding also shortens the processing time and improves the efficiency. The wood composition and microstructure of different wood species are different, and the performance difference of wood species has great influence on wood welding (Belleville & Stevanovic, 2012).

Figure 1-5 Furniture made by welding wood

(Source: https://www.contemporist.com/welding-wood-by-culdesac/).

1.2 Objective and scope of work

The overall objective of this study was to study the mechanical performance of wood welding technique in timber structural components.

The specific objectives were to:

(1) observe the failure mode of a wood welded connection specimens; and

(2) examine and compare the mechanical properties of welded wood connection specimens with those made via push-in and bolting methods.

To reach these objectives, the following testing work was conducted:

(1) The joint tests were conducted using a universal mechanical testing machine;

(2) moisture content of the specimens was tested at the end of joint test; and

(3) specific gravity of the specimen was tested by using immersion method.

1.3 Outline of thesis report

The material presented in this report is organized into five chapters.

Chapter 1 states the project background, development status, and problem statement.

Chapter 2 gives a general introduction to wood welding, and reviews literature for definition and classification, chemical reactions during process, influence factors of welding strength and modeling.

Chapter 3 presents the materials and methods. The S-P-F lumber and sugar maple dowel were used as test materials. A total of six sets of connection types were made by taking into account, dowel types (maple dowels and metal bolts), loading directions (parallel and perpendicular), and methods for making connection specimens ((push-in dowel, welding dowel, and bolted). In addition, the moisture content and specific gravity of selected specimens were measured.

Chapter 4 discusses the load-slip curves and failure types of the connection specimens tested and discusses, their mechanical properties, and uses the EYM model to discuss the results.

Chapter 5 summarizes the conclusions and recommendations derived from this study.

2 Literature Review

2.1 Wood welding

2.1.1 Definition and classification

Wood welding is a technique in which the heat needed to melt the material is generated by pressing one of the samples to be jointed through a displacement or rotation. For thermoplastic materials, such bonds are permanent and have a strength approaching that of the parent material (TWI, 2005). The main welding parameters involved in this technology are motion amplitude and frequency, friction pressure and holding pressure duration (Leban & Pizzi, 2007). According to the welding methods, wood friction welding can be divided into linear vibration welding and rotational dowel welding.

Linear welding means applying pressure on the surface of the wood, the two wooden components reciprocate in a linear friction motion with a certain amplitude and frequency (Figure 2-1). The joint tensile strength depends on vibration amplitude and welding pressure. The higher the welding pressure in the range used, the higher bond strength of the joint. Meanwhile, the tensile strength also is influenced by welding time, but the effect is relatively small (Gfeller & Zanetti, 2003).

Rotational dowel welding is to insert the rotating tenon into the reserved borehole under a certain pressure to form a molten interface for welding (Figure 2-1). When the fusion and bonding process is complete, rotation is stopped, or the pressure increase ceases and it is

maintained for a short period of time. The species used to make dowels are usually high-density hardwoods (Leban & Pizzi, 2007).

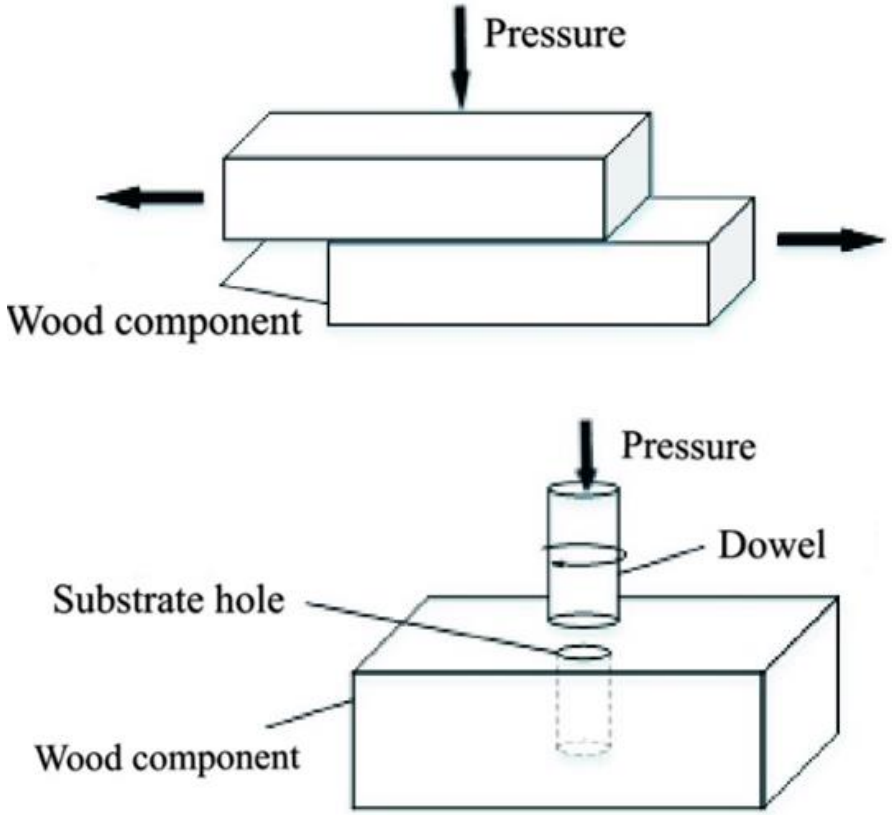

Figure 2-1 Schematic diagram of the two wood welding methods: linear (upper) and rotational (lower) (Source: https://kns.cnki.net/kcms).

2.1.2 Chemical reactions during welding

2.1.2.1 Chemical reactions

The glass transition temperature T_g of the lignin in the matrix is approximately 170 °C (338 °F). Above the matrix T_g, it is possible to cause the lignin to undergo thermoplastic flow and, upon cooling, reset in the same or modified configuration (Wood Handbook, 1974).

Mainly melting of lignin is one of the main causes of the bonding observed. In the experiment, the equilibrium moisture content of the samples was 12%, and the temperature of bonding layer reached 170°C. Then the structure was observed under a scanning electron microscopy (SEM). Entanglement network encased in a matrix of molten intercellular material, mainly lignin, that has subsequently solidified on cooling constitutes the joint's bond-line. The main cause of wood fusion welding might be a physicochemical effect rather than a chemical cross-linking reaction (Gfeller & Zantti, 2003).

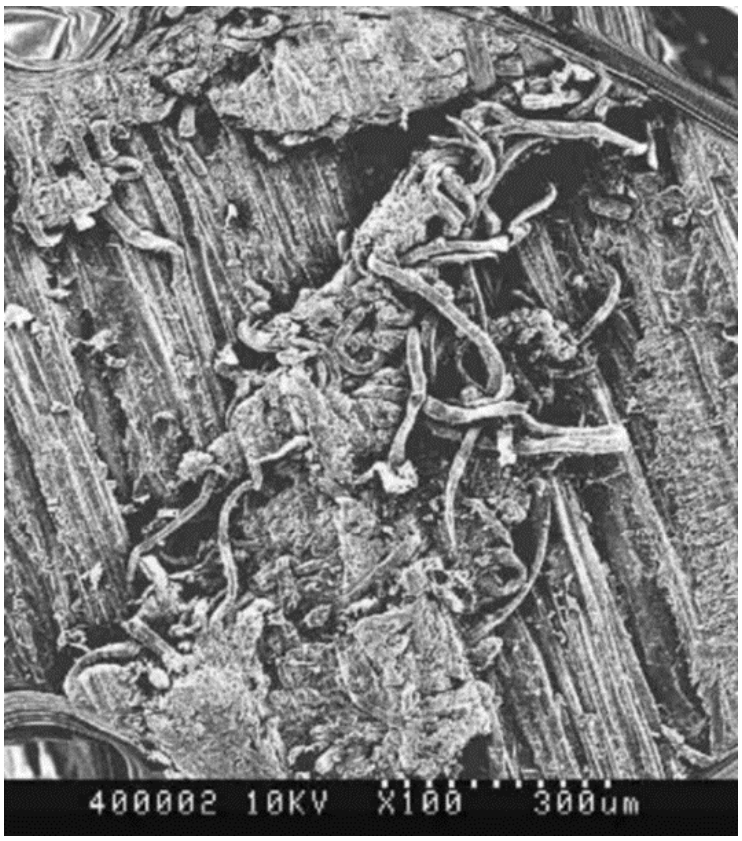

Figure 2-2 Scanning electron microscopy images of lignin fusion band with cellulose fibers and wood cells (Source: Gfeller & Zantti, 2018).

Most of the chemical reactions involved in wood welding occur at the beginning of the process, leading to furfural production and extensive degradation of hemicellulose. At this stage, only a small part of cellulose degrades and lignin fuses. At the same time, wood pyrolysis produces charcoal. The lignin then cross-links and forms a complex network (Cornault & Carpentier, 2020).

2.1.2.2 Chemical composition of volatiles

Wood welding produces smoke during welding while there are no emissions at all after welding ends. Analysis of the gases, vapour and degradation volatiles emitted as smoke by the welding interface during welding has shown that the compounds in such a smoke are water vapour, CO_2, degradation compounds from wood polymeric carbohydrates and from amorphous lignin, as well as some volatile terpenes. Furthermore, the quantity of CO_2 emitted is very low, and neither CO nor methane is emitted (Omrani & Masson, 2012).

Rotation welding produces less smoke than linear welding. These differences mainly focus on welding time and the maximum temperature achieved during welding. Rotation welding reaches a low maximum temperature of 183 ºC, while linear welding can reach as high as 230 ºC (Zoulian & Pizzi, 2006). Lower temperatures and shorter times may account for lower smoke levels during rotation welding.

2.1.3 Influence factors of wood welding strength

2.1.3.1 Materials

2.1.3.1.1 Wood species

Belleville and Pizzi (2012) examined the species effect on the dowel withdrawal strength with the aim of identifying the optimized species combination. The species used were sugar maple (*Acer saccharum Marshall*) and yellow birch (*Betula alleghaniensis*).

In Belleville and Pizzi (2012) experiment, dowels made of one species were welded into wood slats of another species and vice versa. The wood material was pre-conditioned under a 20°C temperature and 60% relative humidity environment until the specimen reached its constant mass. Other experimental welding conditions remained unchanged. The optimal welding mechanical properties were determined from the dowel withdrawal strength using a standard tensile strength test (ASTM D1037) on a universal testing machine.

The experiment demonstrated that the performance of sugar maple was better than that of yellow birch when the dowel and substrates were welded with the same wood species. The welding performance was better when birch wood was used as the base material and sugar maple as the dowel (Belleville & Pizzi, 2012).

Substrate	Dowel	Welding parameters	Number of replicates
Sugar maple	Yellow birch	Optimized sugar maple parameters	12
Sugar maple	Yellow birch	Optimized yellow birch parameters	12
Yellow birch	Sugar maple	Optimized sugar maple parameters	12
Yellow birch	Sugar maple	Optimized yellow birch parameters	12

Table 2-1 Test design summary for species combinations

(Source: Belleville & Pizzi, 2012).

2.1.3.1.2 Diameter ratio between wood dowel and pre-drill hole

Rodriguez and Diouf (2012) aimed at investigating the possibility to apply high-speed rotation-induced wood-dowel welding technique to two Canadian hardwood species commonly used for furniture and structural applications, sugar maple and yellow birch. Different factors had been evaluated such as the wood species, the grain orientation, as well as the ratio between wood dowel and pre-drill diameter.

Commercial smooth wood dowels of birch and maple woods, dried at 12% moisture content, 9.68mm in diameter and 80mm in length, were inserted using a high-speed fixed-base drill, with pre-drilled holes of various diameters (7.14,7.37 or 7.67mm), in pieces of birch woods (40×20×20mm), respectively. The welded samples were conditioned for at least one week in an environmental chamber at 20ºC and 65% relative humidity before testing. The tensile strength of welded components was tested (Rodriguez & Diouf, 2012).

The experimental results show that the ratio of mortise diameter to pre-drilling has an effect on the tensile strength of welded specimens. The greater the ratio, the greater the tensile strength (Rodriguez & Diouf, 2012). The larger the aperture gap was, the lateral pressure of the mortise on the hole wall would be increased, the friction effect would be enhanced, the temperature of the welding surface could be accelerated, and more materials could be provided for the welding process, so that the welding effect was better (Zhu & Chen, 2019).

2.1.3.1.3 Wood grain orientation

Zhu and Chen (2019) tested the rotary welding of dowel joints with different substrate grain orientations, and compared with the impact test specimens, analyzed its effect on the tensile force of welded specimens.

Both the substrate material and dowel were made of Korean pine (*Pinus koraiensis Sieb. Et. Zucc*). The size of the base material was 40mm, the pre-drilled aperture of the base material was 8mm, and the depth was 40mm. The length and diameter of the wood dowels were 100mm, and 10mm, respectively. The substrate insertion direction was divided into two types: parallel to grain and perpendicular to grain. The moisture content of the experimental material was adjusted to 8%. The dowel was inserted into the substrate material at a high speed with a rotation speed of 2500r/min and an insertion speed of 15mm/s. The pull-out tension tests were carried out on the wood welded specimens (Zhu & Chen, 2019).

By observing the welding state of the two groups of specimens, it could be found that the shape of the wood dowel was different. In parallel to grain group, the diameter of wood dowel decreased along the insertion direction, and its diameter changed continuously. For perpendicular to grain group, the diameter of the dowel was greatly reduced along the insertion direction, and the diameter changed dramatically within 5mm of the last friction involved.

Figure 2-3 Wood dowel of parallel to grain welding (Source: Zhu & Chen,2019).

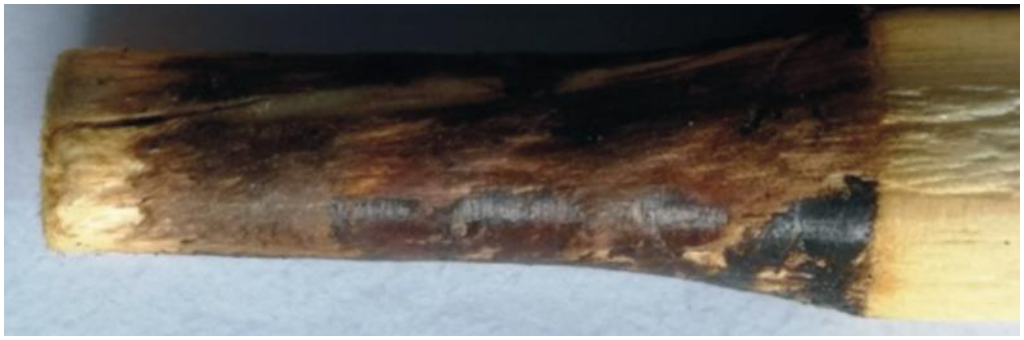

Figure 2-4 Wood dowel of perpendicular to grain welding (Source: Zhu & Chen,2019).

Perpendicular to grain welding has a greater weakening effect on the diameter of the wood dowel, and more material loss in the welding process has a negative impact on the welding strength (Zhu & Chen, 2019).

2.1.3.1.4 Pretreat wood dowel with copper chloride ($CuCl_2$)

Zhang and Gao (2018) examined the temperature distribution and pull-out resistance during rotation welding process using birch (*Betula spp.*) wood dowel and Chinese larch (*Larix gmelinii*) substrates.

The wood dowels were divided into two categories including an untreated group and a pretreated group. The yellow birch was used as dowel, and Chinese larch (Larix potaninii) was used as substrate. The wood dowels of the pretreated group were immersed in 0.1mol/L $CuCl_2$ solution for 30min. Temperature test, pull-out test, and thermogravimetric (TG) analysis were performed on each specimen.

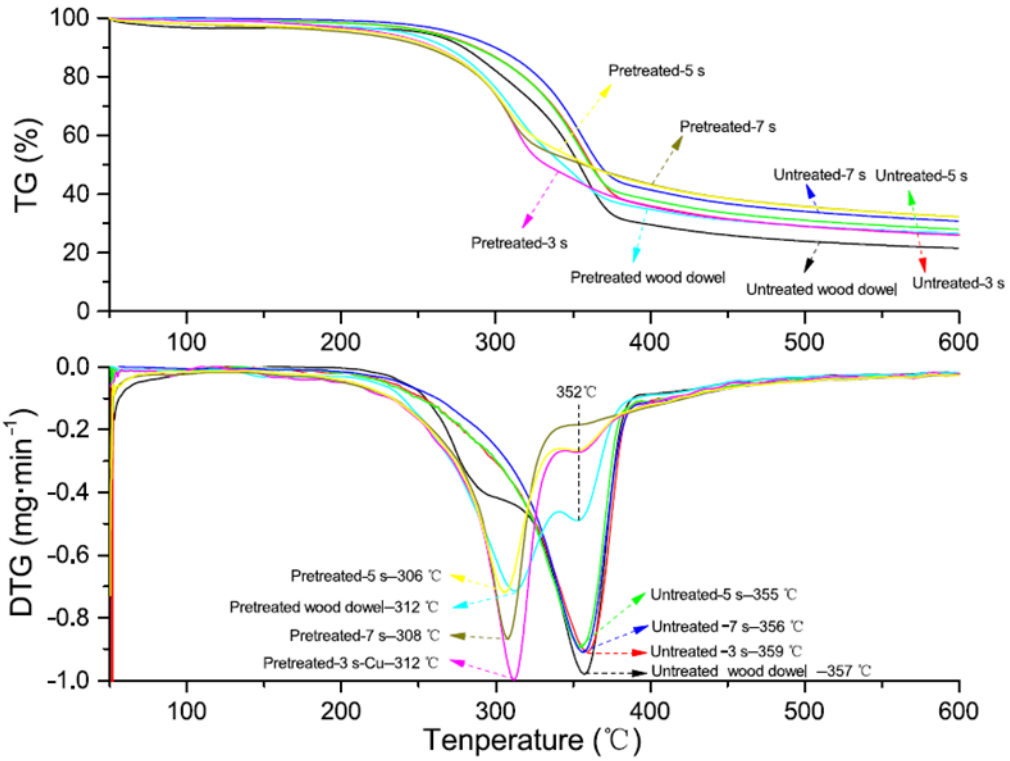

Figure 2-5 TG/DTG curves of wood dowel and welding interface

(Source: Zhang & Gao, 2018).

The pretreatment of wood dowel with $CuCl_2$ could effectively improve the pullout resistance of wood dowel welding. The pretreated group's pull-out test results were 68.28% higher than untreated group. Meanwhile, the residual ratio of dowel in pretreated group was 6.8% higher than untreated group. TG analysis showed that the enhancement mechanism of wood dowel pretreated with $CuCl_2$ that resulted from acid hydrolysis of hemicellulose and cellulose of wood dowel, which occurred during the process of $CuCl_2$ immersion. This method promoted the formation of more molten materials by the depolymerization and pyrolysis of the wood constituents (Zhang & Gao, 2018).

2.1.3.1.5 Pretreat wood dowel with sunflower oil

Segovia and Zhou (2012) pre-oiled the dowels with sun-flower oil to study the effect of pretreatment on the mechanical properties and water resistance of wood welding.

In the experiment, wooden pins, which were dried to 2% moisture content and 10 mm in diameter and 190 mm in length, were soaked in sunflower oil for 10 minutes. The treated pins are then inserted along the edge of the board for welding. The wooden pins were added and fixed to the wood blockboards as shown in the figure, and 20 joinery board plates were made in this way. The three-point bending test was performed on the panels to record the deformation diagram and the maximum breaking strength of the components (Segovia & Zhu, 2012).

The wooden dowels pretreated with sunflower oil immersion showed several advantages as follows:

1. They were easier to insert into the pre-drilled substrate.
2. The lubrication of the oil slowed the welding process and allowed the dowel to be inserted deeper so that more layers of wood could be connected with the same dowel.
3. Oil pretreated dowels could be used to connect untreated dowels in fewer quantities, thus it could save processing time and materials.
4. Oil treatment of welded joints could make them have higher wettability.

Figure 2-6 Beech wood dowels soaking in sunflower oil

(Source: Segovia & Zhu, 2012).

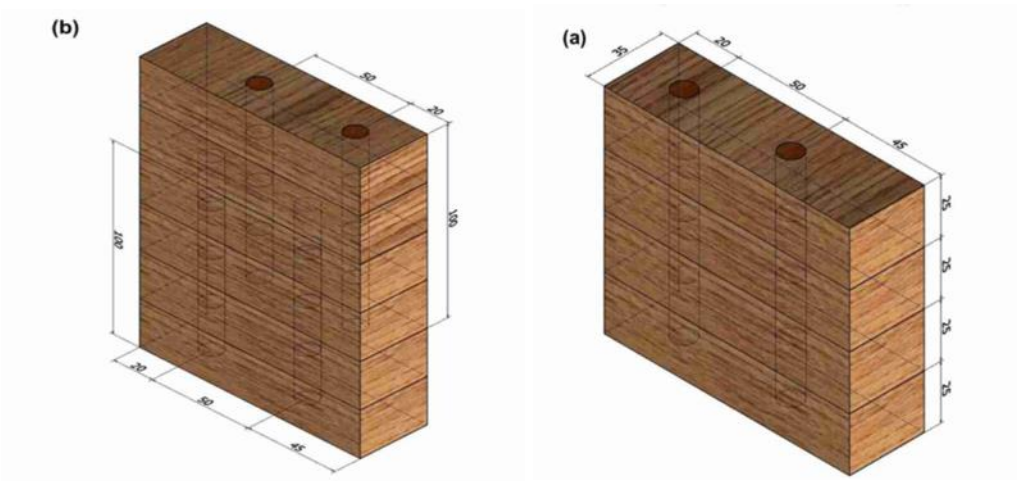

Figure 2-7 Insertion scheme of oiled dowels through four layers of wood substrate: (a) first two dowels and (b) the first and second two dowels in place (Source: Segovia & Zhu, 2012).

2.1.3.2 Machining parameters

2.1.3.2.1 Rotational speed

Belleville and Pizzi (2012) aimed at defining the optimal wood-dowel welding parameters for two North American hardwood species frequently used for indoor appearance products: sugar maple (*Acer saccharum*) and yellow birch (*Betula alleghaniensis*). The investigated parameters for both species were grain orientation, rotational speed, and insertion speed.

The experimental environment used the same conditions as the wood species experiment. The tensile strength of each specimen was measured by changing the rotating speed. When the tenon and the base material were welded to the same species, the tenon speed was usually 1000, 1500r/min and 2500r/min. The optimum rotational speed of sugar maple and birch was 1000r/min, with tensile strength reached 1.84-2.15KN. High speed could lead to the welding interface temperature rise too fast, interface coking and strength reduction. When the speed reached 4000-4500r/min, the tensile strength dropped to 1.5 KN (Belleville & Pizzi, 2012).

Rotational speed (rpm)	Sugar maple		Yellow birch	
	Mean $T \pm$ SE (°C)	Max T (°C)	Mean $T \pm$ SE (°C)	Max T (°C)
1000	244.1 (12.4)	303	282.6 (10.5)	337
1500	281.1 (11.1)	326	297.4 (8.5)	333
2500	328.6 (9.8)	380	327.3 (16.7)	371

Table 2-2 Experimental results for peak temperature (T) during rotational wood-dowel welding (Source: Belleville & Pizzi, 2012).

Pu (2019) examined the optimal rotational welding parameters for producing high-strength wood joints using the Response Surface Methodology. Black spruce (*Picea mariana*) was used as substrates; sugar maple (*Acer saccharum*) and hickory (*Carya spp.*) were used as dowels of a diameter of 19 mm (0.75 inch). The push-out tests were conducted using a universal mechanical testing machine. The effects of each parameter and their interactive effects on the maximum push-out load (P_{max}) and stiffness (K) of joints were examined. It was found that the optimum welding rotational speed was 900 rotation per minute.

2.1.3.2.2 Insertion speed

Auchet and Segovia (2010) studied whether the dowel insertion speed accelerating or constant could determine parameters for the tensile strength of welded dowel joints.The welded samples were conditioned for one week in an environmental chamber (20°C and 65% RH). The samples were tested in tension with an insertion universal testing machine at a rate of 2 mm/min. When the tenon and the substrate are of the same species, the optimum insertion speed of sugar maple was 25.0mm/s and 16.7mm/s for birch. Tensile strength reached the max (4,700N/mm²) when the insertion rate was 18-20mm/min and welding time was 1.2s (Auchet & Segovia, 2012).

At the same time, the relationship between initial velocity and acceleration was also found. When the initial speed of the dowel was low, better tensile strength can be obtained by accelerating the insertion. When the initial speed was high, the constant insertion speed can achieve better performance (Auchet & Segovia, 2012).

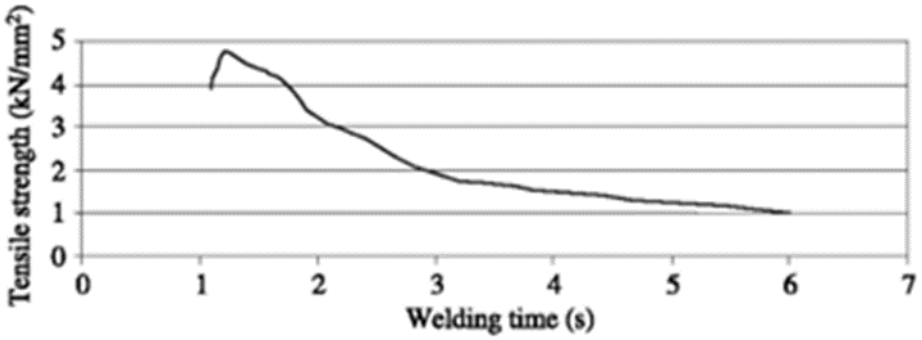

Figure 2-8 Tensile strength as a function of welding time at constant dowel insertion time (Source: Auchet & Segovia, 2012).

2.1.3.2.3 Insertion angle

Belleville and Segovia (2011) dealt with the preparation of blockboard panels by rotational dowel welding and tested their mechanical performance using Commercial beech (*Fagus sylvatica*) wood fluted dowels, dried to 2% moisture content. The samples were tested in three-point bending at a constant rate of 2mm/min with testing machine Instron 4467 30KN(UK). Their results indicated that 20° dowel insertion angle the samples showed a significant improvement in tensile strength over the 10° and 0° insertion angle cases. A serious of samples were tested in three-point bending at a constant rate of 2 mm/min with a universal testing machine according to ASTM D1037 “Standard Test Method for Evaluating Properties of Wood-Base Fiber and Particle Panel Materials.”

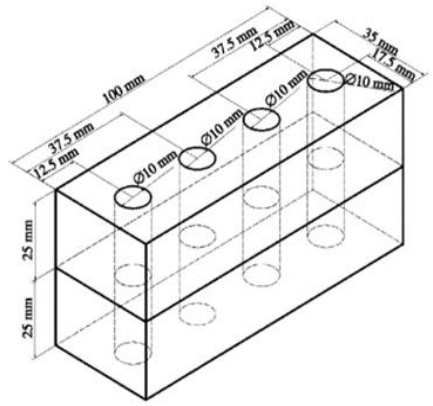

(a)

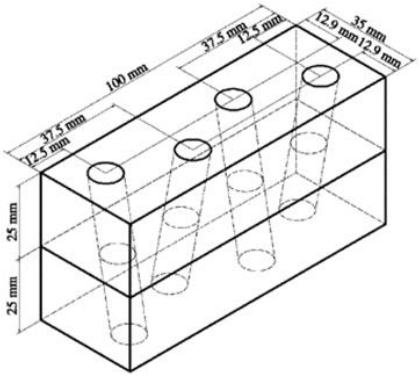

(b)

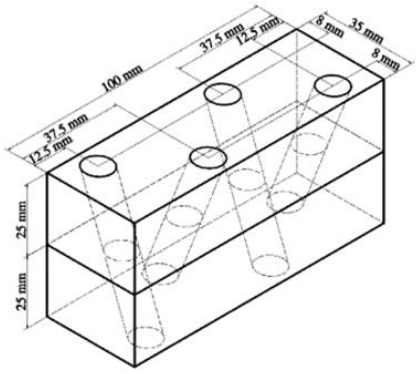

(c)

Figure 2-9 Schematic representation of the pattern of dowel insertion (a) at 0° insertion angle, (b) at 10° insertion angle and (c) at 20° insertion angle (Source: Belleville & Pizzi, 2012).

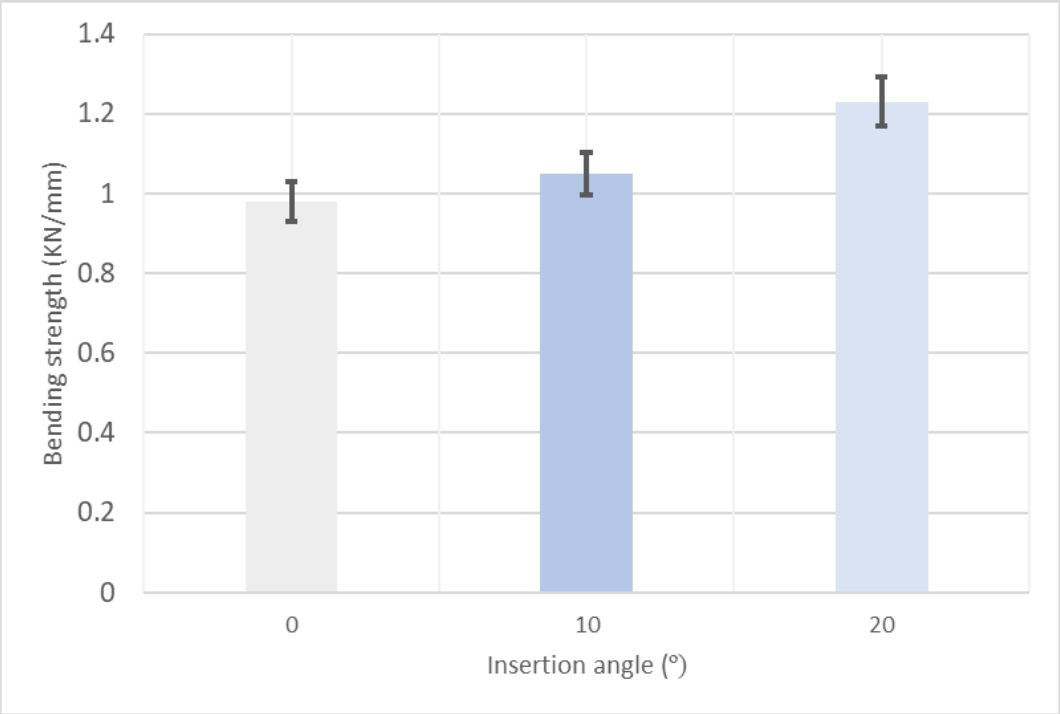

Figure 2-10 Means and standard deviations of the bending strength of dowel welded blockboards.

Meanwhile, slanting the dowel into the substrate increased the shear stress compared with vertical insertion. On the other hand, slanting insertion had a larger contact area than vertical insertion at the same depth (Belleville and Pizzi, 2012).

2.1.4 Modeling

2.1.4.1 A heat-transfer model in wood welding

Zoulalian and Pizzi (2006) modelled the relationship between temperature, time of friction and thermal flux for high-speed rotational wood dowel welding through a heat-transfer model. They established a function relationship between interface temperature and friction time of rotational dowel welding.

$$\hat{T} = \frac{2\beta\sqrt{\alpha}}{h}\tau u\sqrt{\frac{t}{\pi}}.$$

Where, τ-the friction stress, μ-the rate of rotation or vibration, β-the fraction of mechanical energy convertible into thermal energy, and where *h* and α were, respectively, the thermal conductively and diffusivity of the wood (Zoulian and Pizzi, 2006). For both rotational dowel welding and linear welding systems the value of β was found to be 0.080±0.01. The results obtained for rotational dowel welding indicated that a temperature of 183°C was optimal for rotational welding. They found the optimal welding temperature for each wood species as follows.

Species	European beech	Sugar maple	Yellow birch
Optimum rotational welding temperature (℃)	183	244	282

Table 2-3 Optimum rotational welding temperature table for three species

(Source: Zoulian & Pizzi, 2006).

2.1.4.2 Finite element simulation

Oudjene and Khelifa (2012) developed numerical models, using a 3D finite element analysis method, for simulating the behavior of dowel-welded wood joints. Simulation results for step butt wood joints with two welded wood dowels under shear were analyzed and a good agreement with the experimental results was found.

The finite element method can simulate the failure behavior of wood welded joints. Numerical models using a 3D finite element analysis method and the behavior of dowel-welded wood joints are presented. Simulation results for step butt wood joints with two welded wood dowels under shear are analyzed and a good agreement with the experimental results is shown.

The two wood pieces were made of beech wood, with pre-drilled holes of 8mm diameter and dimensions of 190×38×38(mm). They were assembled using commercial beech wood fluted dowels, 8cm long and 10mm in diameter. Ten joints were tested in tension on an Instron4467 testing machine at a crosshead speed of 5mm/min.

The coulomb friction model with a friction coefficient of 0.1 was used to simulate the interaction of the contact surface, assuming that the interface was completely welded. The results show that the simulation results under shearing condition are in good agreement with the experimental results, and the simulation model could effectively simulate the nonlinear behavior of welding failure (Oudjene & Khelifa, 2012).

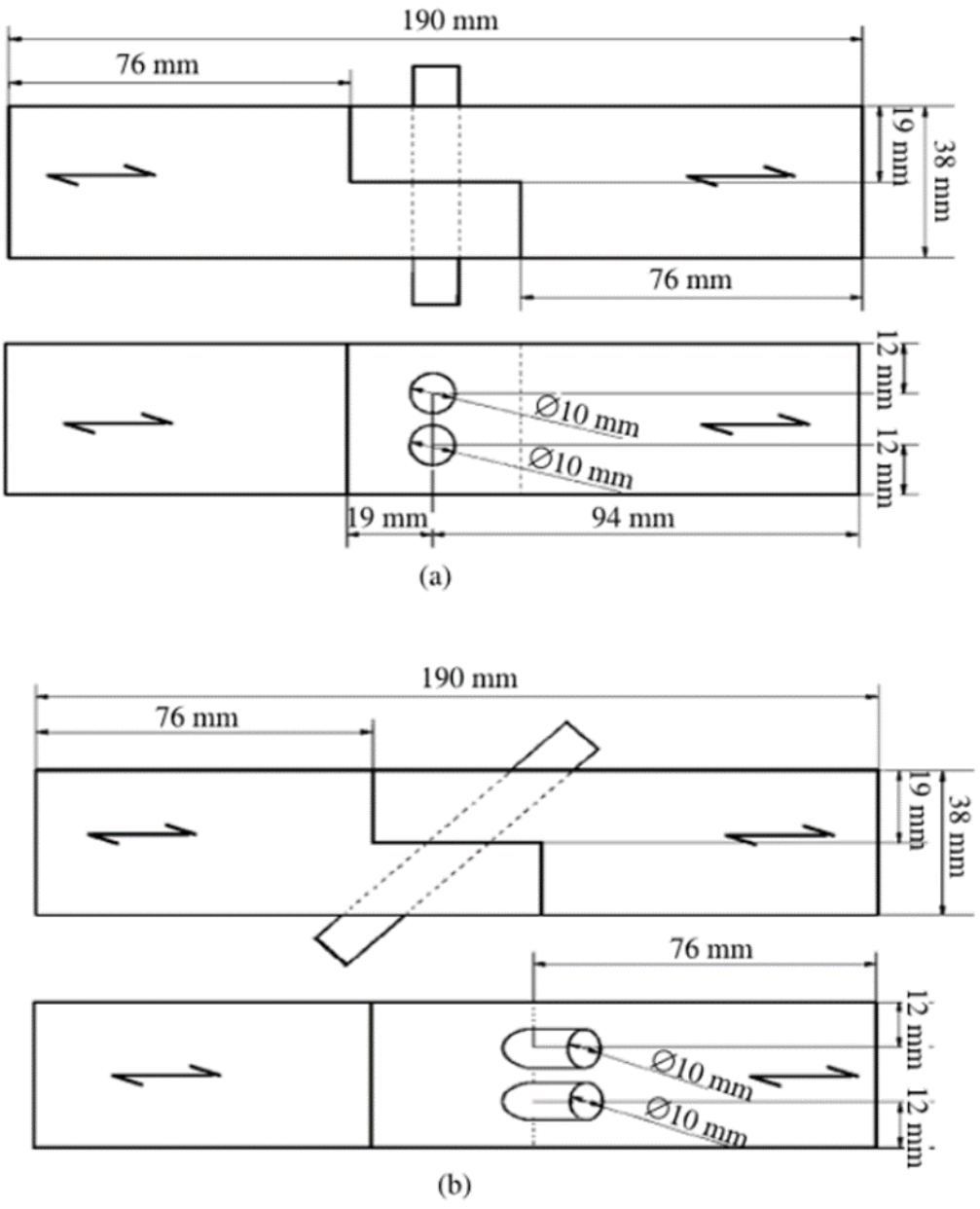

Figure 2-11 Schematic illustration of the dowel-welded wood joints: (a) at 90º insertion angle, and (b) at 45º insertion angle (Source: Oudjene & Khelifa, 2012).

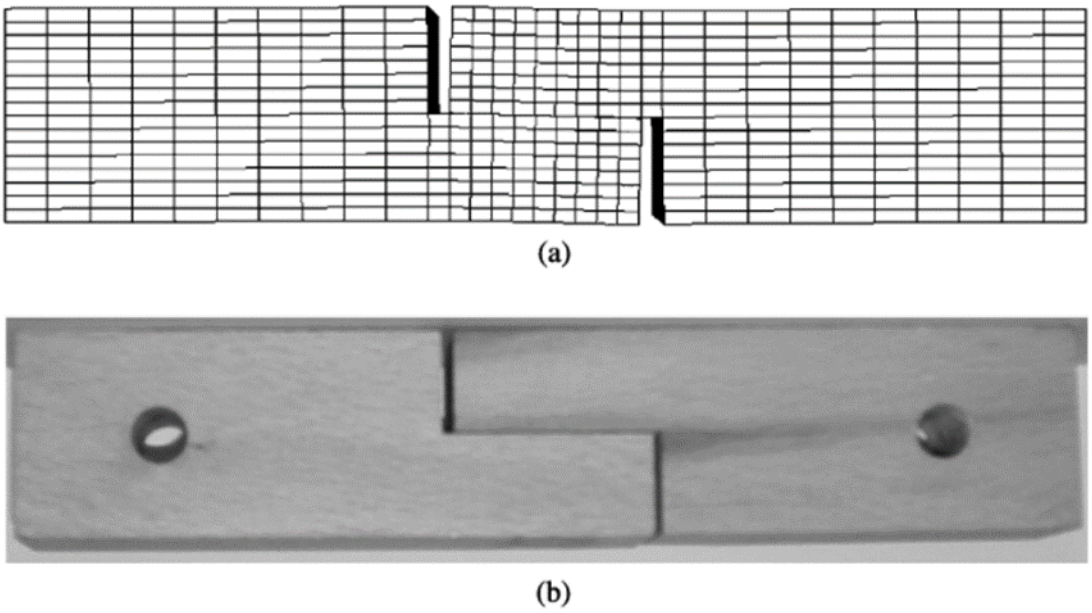

Figure 2-12 Deformed joints at failure (dowels at 90 insertion angle): (a) simulation and (b) experiment (Source: Oudjene & Khelifa, 2012).

2.1.4.3 European Yield Model

The European yield model (EYM) (Johansen, 1949) has been adopted as a base for setting allowable strengths for dowel-type connections. It is the basis of all timber design standards across the world for predicting ductile modes of failure of connections containing dowel type fasteners: nail, wood screw, lag screw, bolt, and steel dowel.

The EYM assumes that the ultimate bearing capacity of a bolted connection is attained when: Three types of failure mechanisms were observed in a double-shear connection (Johansen, 1949), which are illustrated in Figure 2-15, i.e., Mode I without any plastic hinge (with a double-shear connection and a stiff dowel), Mode II with one plastic hinge (with a low stiffness dowel bent in the middle timber member of a double-shear connection), and Mode III with plastic hinges form in both side and main members. In the structural engineering the term, "plastic hinge" is defined as the deformation of a section of a beam where plastic bending occurs (Megson, 2005). These assumptions provide for several modes of yielding of connection depending on member dimensions, member strength, and bolt strength.

Yield modes, together with formulas for the yield strength Z_y corresponding to each failure mode, are displayed in Figure 2-14 for three- and two-member connections, respectively. Where d_F is nominal diameter of fastener; t_1, t_2 is bearing strength of fastener in members and 2; f_1, f_2 is embedment strength of member 1 and 2; and f_y is yield strength of fastener in bending.

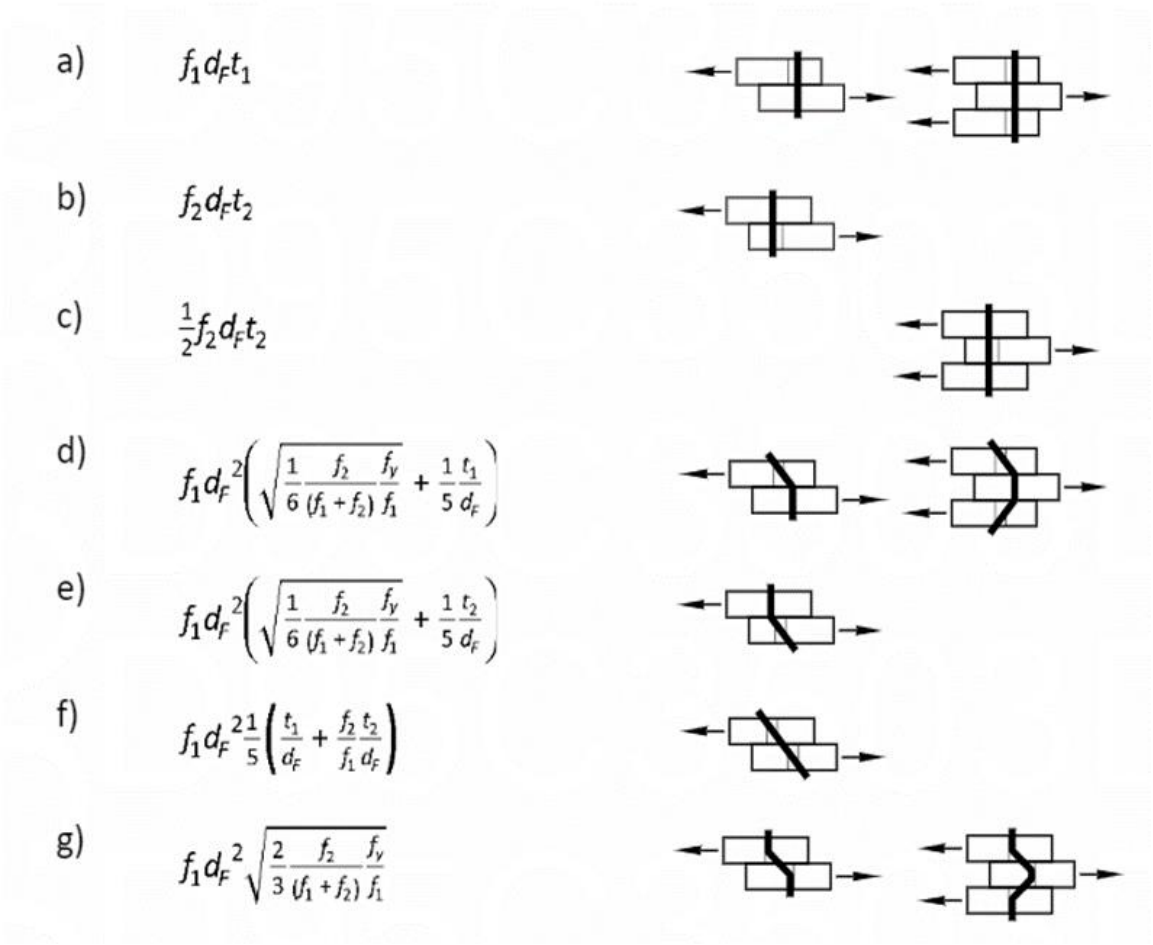

Figure 2-13 European Yield Model (Source: CSA, 2012).

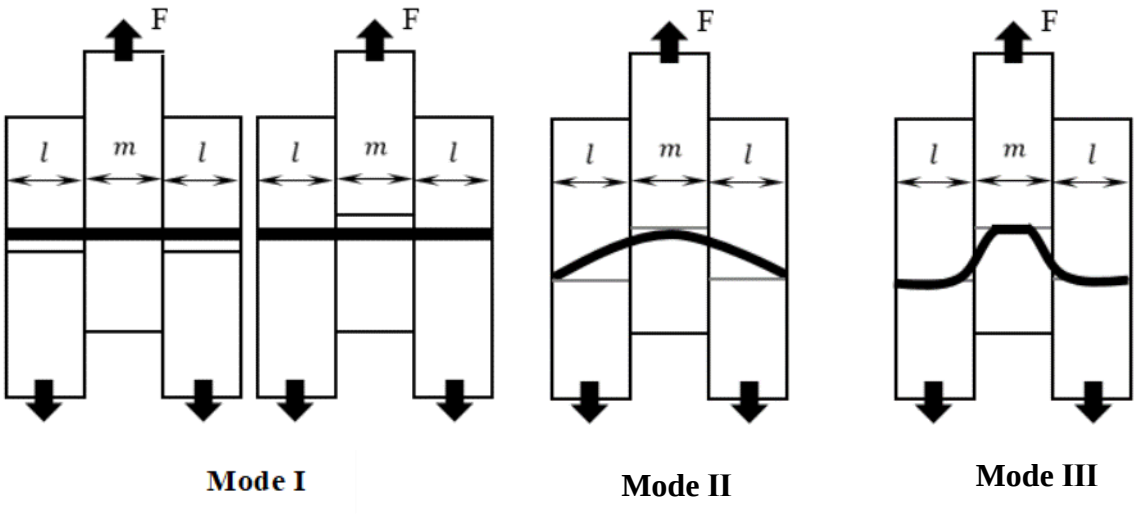

Figure 2-14 Failure mechanisms for double-shear connections (Source: Johansen, 1949)

2.2 Summary and problem statement

Wood welding, an efficient, green, and pollution-free process, can be used as an environmentally friendly technique for interior decoration and potential structural application. Wood welding has a wide application prospect in the future because of its good dry bonding strength. For example, rotational dowel welding can repair and reinforce ancient buildings.

In this regard, the technical review suggests that there are following methods of improvement.

1. *Development of rotational welding equipment.* At present, the existing wood welding equipment is mostly confined to the laboratory. A kind of automatic and industrialized welding equipment is very important to the development of wood welding technology.
2. *Improvement of welding performance*. In order to apply wood welding to the structure, the strength of the welded members needs to be increased and their sensitivity to the external environment needs to be reduced.
3. *Research on new friction welding.* Scientists are currently investigating the potential of ultrasonic and micro-friction stir welding.
4. *Pre-treatment of wood pins with copper chloride.* This can improve the pull-out resistance of wood components, but as a chemical substance, copper chloride is not the best choice, because it will cause some pollution to the environment. In the future research, it should be further developed to substitute environment-friendly substances for copper chloride.

In short, wood welding technology shows excellent performance, shows excellent performance; in addition to extending the potential of the wood industry, it offers to reduce environmental pollution, but also can effectively protect the environment.

3 Materials and methods

3.1 Materials

2×6 spruce-pine-fir (S-P-F) lumber (38mm thick and 140mm wide) were selected from one batch of lumber, and then 300mm (12″) and 430mm (17″) clear wood blocks were cut from the center 3-inch part. The sugar maple (*Acer saccharum*) dowels were bought from a local drumstick factory in Fredericton, New Brunswick, Canada. The length and diameter of each dowel were 457mm (18″) and 19mm (3/4″), respectively. Each dowel was crosscut into two 170mm (6-11/6″) dowels. 6 metal bolts of the same diameter were obtained from the Wood Science and Technology Centre, University of New Brunswick, Fredericton, Canada. The total length of sawn lumber required for the experiment was 48.5m (159ft), and the total length of wood dowel was 5.8m (19ft). Wood blocks and sugar maple dowels were pre-conditioned until their masses reached constant in the conditioning chamber of a temperature of 20˚C and relative humidity (RH) of 65% prior to making joint specimens.

3.2 Design of experiments

3.2.1 Design of test groups

The experimental dowels and substrates were randomly divided into three sets according to the connection type, which were welded, push-in connection with wood dowel, and bolted connection. Two groups of components were separately connected using two connection types in terms of loading direction, i.e., parallel to grain and perpendicular to grain. Six replicates were prepared for each set, generating a total of 36 joint specimens.

3.2.2 Design and fabrication of specimens

For joints involving metal or other side members, the thickness shall be that anticipated in service. For all-wood joints, the thickness of each side members was at least one half of the thickness of the center member, and width and length of all members were selected with regard to the edge and end distances required for a specific application (ASTM, 2012). Therefore, the thickness of the center member of each specimen was 70mm, and the thickness of two side members was 35mm. For perpendicular type test, a clear distance shall be maintained between the supports of at least three times as large as the depth of the transverse member (ASTM,2012).

A metal bolt or wood dowel was placed in the center of the overlapped length. The edge and end distance of the connectors were determined according to the minimum spacing of bolt placement stipulated in CSA O86:19 “Engineering design in Wood” (CSA, 2019).

Symbol	Dimension*	Minimum spacing
S_P	Spacing parallel to grain	$4d_F$
S_Q	Spacing perpendicular to grain	$3d_F$
a	Unloaded end distance parallel to grain	Maximum {$4d_F$, 50 mm}
a_L	Loaded end distance parallel to grain	Maximum {$5d_F$, 50 mm}
e_P	Unloaded edge distance perpendicular to grain	Maximum {$1.5d_F$, 1/2 S_Q}

* d_F = nominal diameter of fastener.

Table 3-1 Placement of bolts and dowels in a connection loaded parallel to grain

(Source: CSA, 2019).

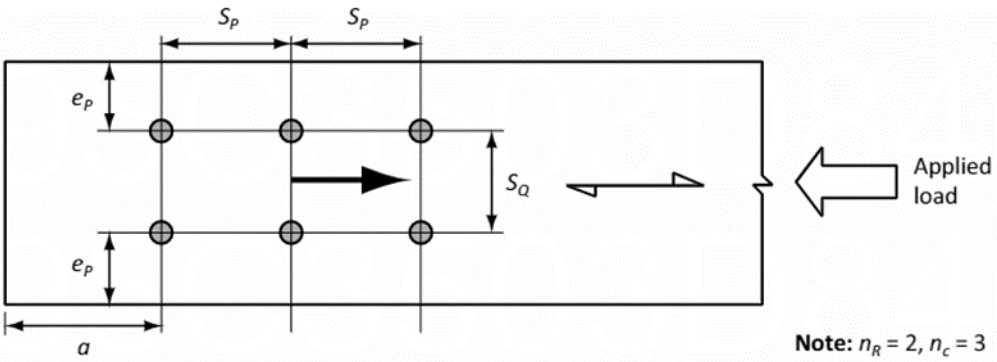

Figure 3-1 Placement of bolts and dowels in a connection loaded parallel to grain in compression load (Source: CSA, 2019).

According to ASTM D1761 “Standard Test Methods for Mechanical Fasteners in Wood” (ASTM, 2012), Bolt-hole diameters were between 0.8 mm and 1.6mm (1/32″and 1/16″) larger than the bolt diameters and holes shall be carefully bored perpendicular to the surface, so that the surface of the hole is smooth and uniform to assure good bearing of a bolt. Therefore, the pre-drilled diameter of the substrate was 20.6mm (4/5″). For welded-hole and push-in-hole diameters, According to Pu (2012), the optimization pre-drill hole diameter and dowel diameter ratio was 0.86, was used for design. Therefore, the hole diameter of the substrate was 16.34mm (16/25″).

Each specimen was coded in such a way (Figure 3-2): The first two letters represent the connection direction between the main member and side member, i.e., parallel (PA) or perpendicular (PE); the second letter represents the way the member was jointed, whether it was Welded, Push-in, or Bolted; and the third letter represents the number in the same group. For example, PA-B-1 means the first bolted specimen tested in the parallel-to-grain direction.

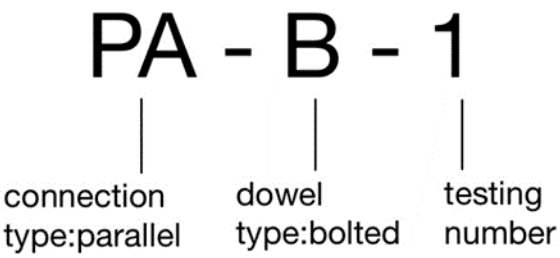

Figure 3-2 Coding system.

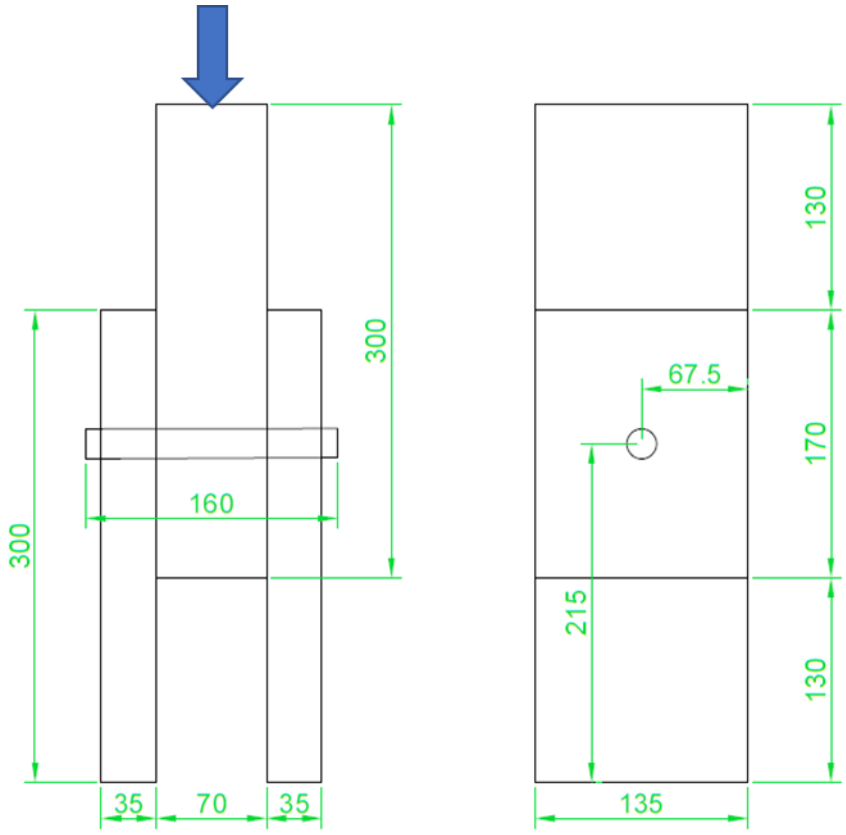

Figure 3-3 Schematic diagram of parallel specimen (unit: mm).

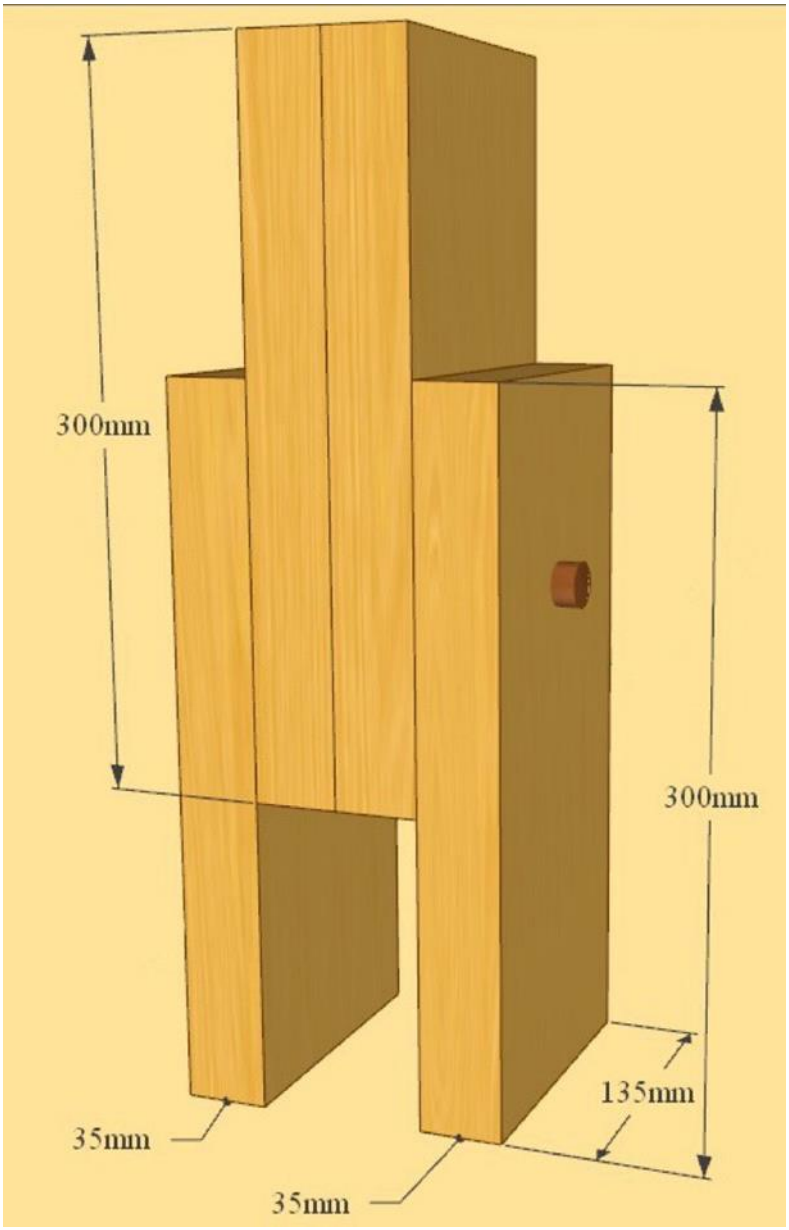
300mm
300mm
135mm
35mm
35mm

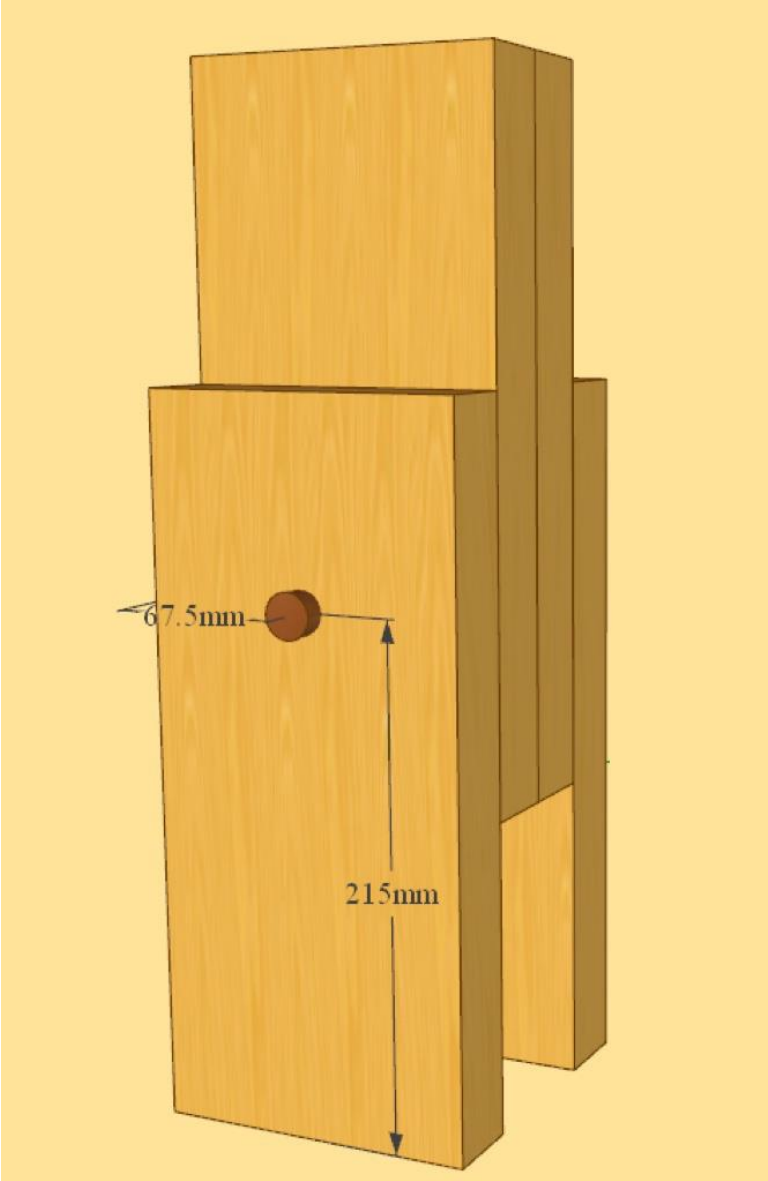

Figure 3-4 Schematic diagram of parallel specimen 3D model.

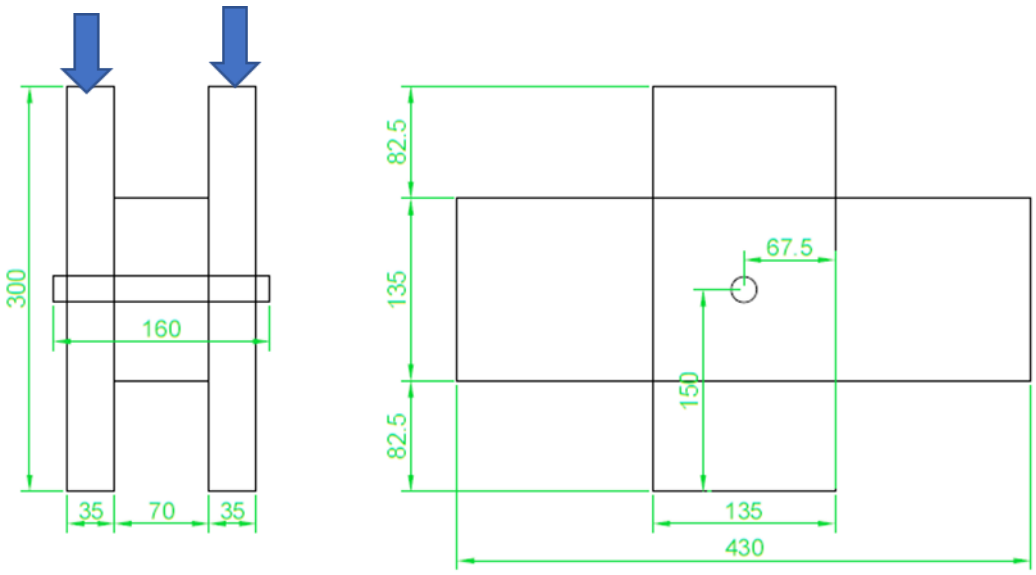

Figure 3-5 Schematic diagram of perpendicular specimen (unit: mm).

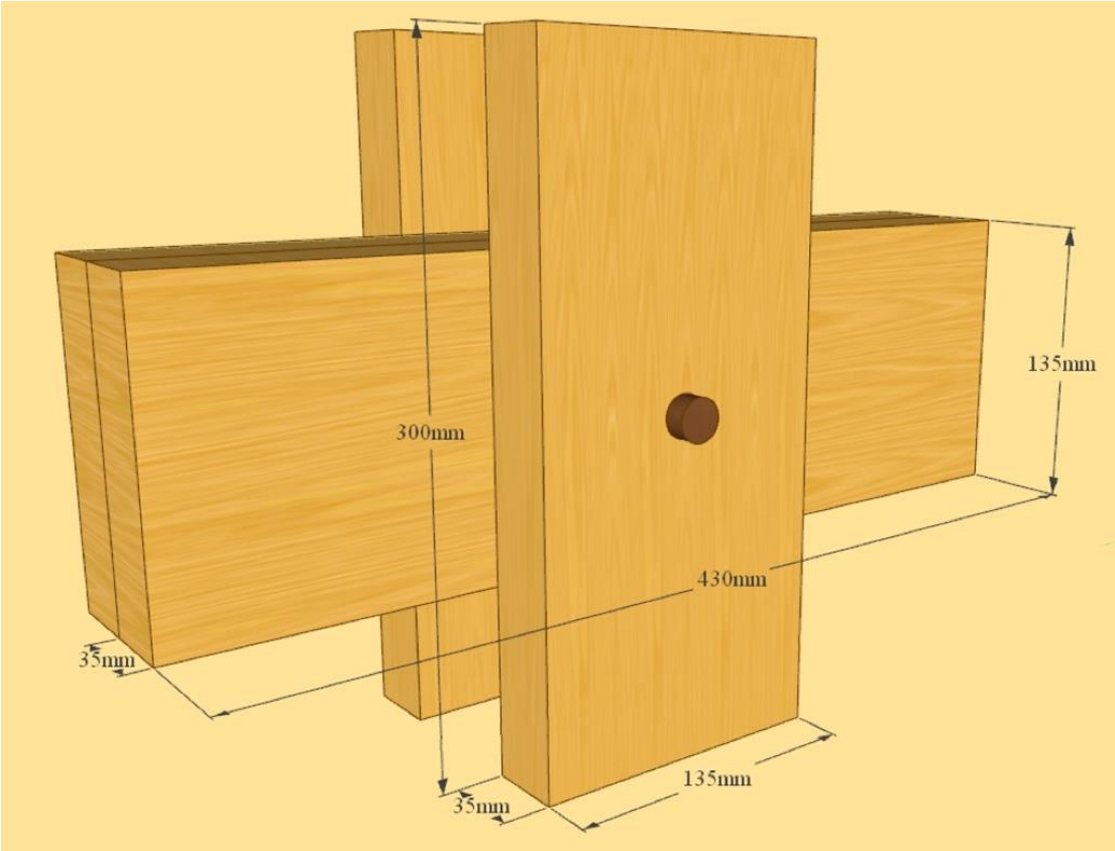
300mm
135mm
430mm
35mm
35mm
135mm

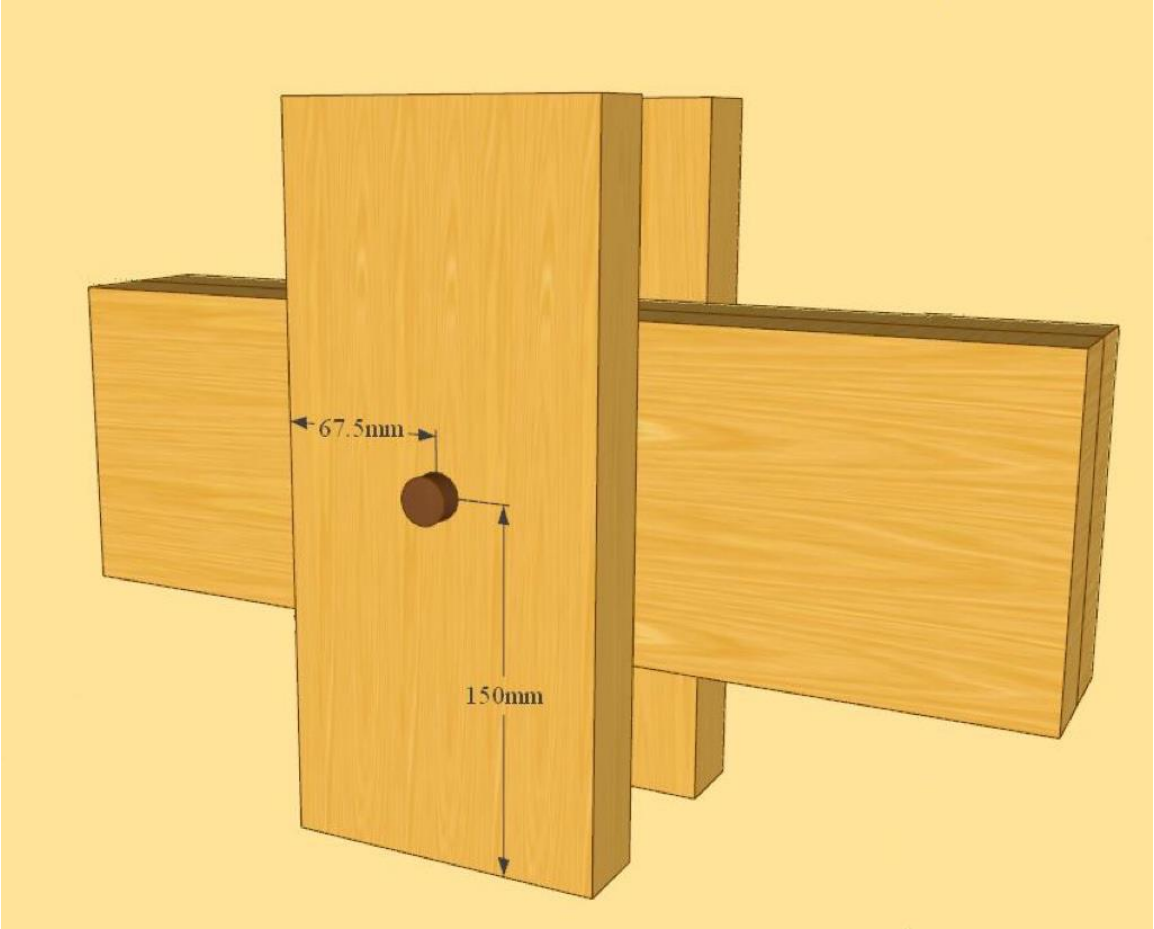

Figure 3-6 Schematic diagram of perpendicular specimen 3D model.

Test Set	Dowel Material	Method	Connection type	Replicates
PA-W	Sugar maple	Welding	Parallel	6
PE-W	Sugar maple	Welding	Perpendicular	6
PA-P	Sugar maple	Push-in	Parallel	6
PE-P	Sugar maple	Push-in	Perpendicular	6
PA-B	Metal	Bolted	Parallel	6
PE-B	Metal	Bolted	Perpendicular	6

Table 3-2 Design of experiment.

3.3 Testing

3.3.1 Joint tests

Before starting the test, all screws fixing the test specimens were removed. Load was applied to the central member along the loading direction (shown in Fig 3-7 and 3-8) using a universal testing machine (Model #: MTS 810) at a rate of 2.5 mm/min. Two Linearly Variable Differential Transformers (LVDTs) were mounted with a hot melt adhesive on the side member to measure the relative displacement between the side member and the center member from the beginning of the application of the load. A build-in data logger was used to record the load, crosshead two LVDTs movement, and elapsed time at a frequency of 2 Hz. The test was continued until the load diminished to 80% of the peak load or severe damage happened. The general behavior of a joint under load was observed and recorded. The first drop of the load indicated, on the testing machine display, the initial possible failure.

Figure 3-7 The perpendicular bolt-connected specimen during test.

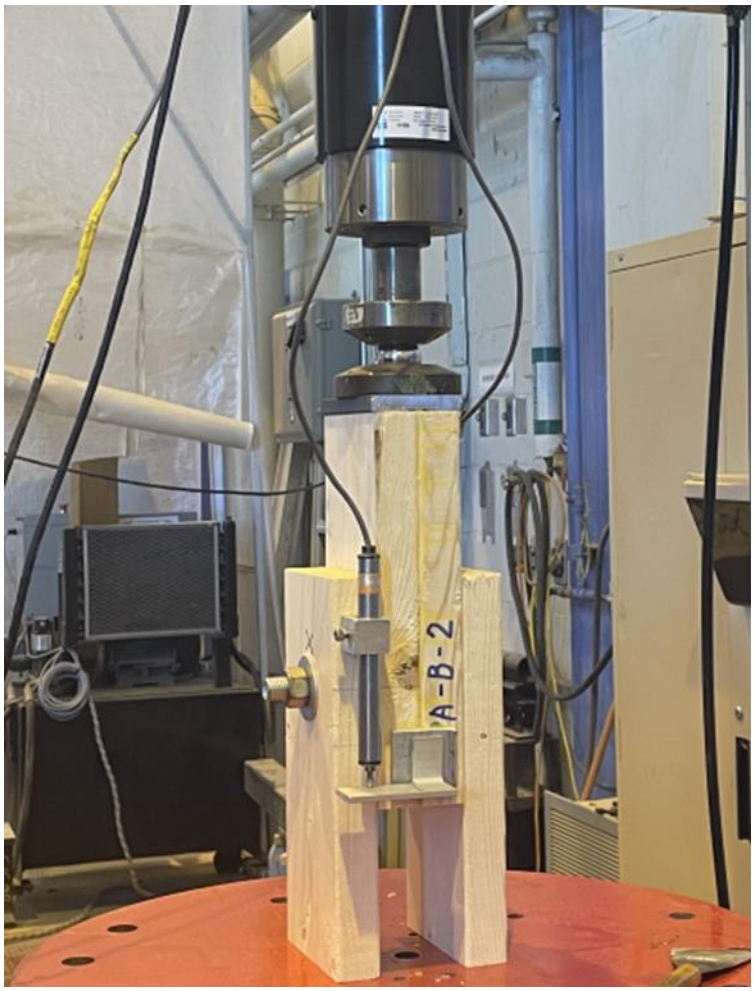

Figure 3-8 The parallel bolt-connected joint specimen during test.

3.3.2 Moisture content test

According to ASTM D4442-20 “Standard Test Methods for Direct Moisture Content Measurement of Wood and Wood-Based Materials” (ASTM, 2016), a moisture section of approximately 25 mm (1 in.) in length was cut from a joint specimen near the point of failure. The cut parts were placed in the oven to dry at temperature of 103 ± 2ºC until approximately constant mass attained, after which the oven-dry mass was determined. The moisture content of the specimen was calculated.

3.3.3 Specific gravity

According to ASTM D2395-17 “Standard Test Methods for Density and Specific Gravity (Relative Density) of Wood and Wood-Based Materials” (ASTM, 2017), the initial mass of wood specimens in air was determined. A container holding enough water to completely submerge a specimen was placed on a balance. Then the balance was set to zero. The specimen was placed using a sharp, pointed, slender rod to completely submerged it in the water without touching the sides of the container. After reaching the equilibrium, the reading on the balance was equal to the mass of water displaced by the specimen.

3.4 Calculations

The mechanical parameters determined in this study are the initial stiffness(K), yield load, peak load, ductility, and energy accumulated at the peak load (W_{peak}) in Figure 3-9. K is defined as the slope of the linear region between 10% and 40% of the peak load. According to ASTM "Standard Test Method for Evaluating Dowel-Bearing Strength of Wood and Wood-Based Products", yield load as the point where the material begins to deviate from ideal elastic to a plastic or pseudo-plastic phase, is calculated via 5% offset method (ASTM, 2018), in which yield load was defined as the intersection of load–displacement curve and the line drawn by offsetting the linear line of 5% of the fastener diameter on the displacement axis. Ductility is defined as the ratio of ultimate displacement to yield displacement.

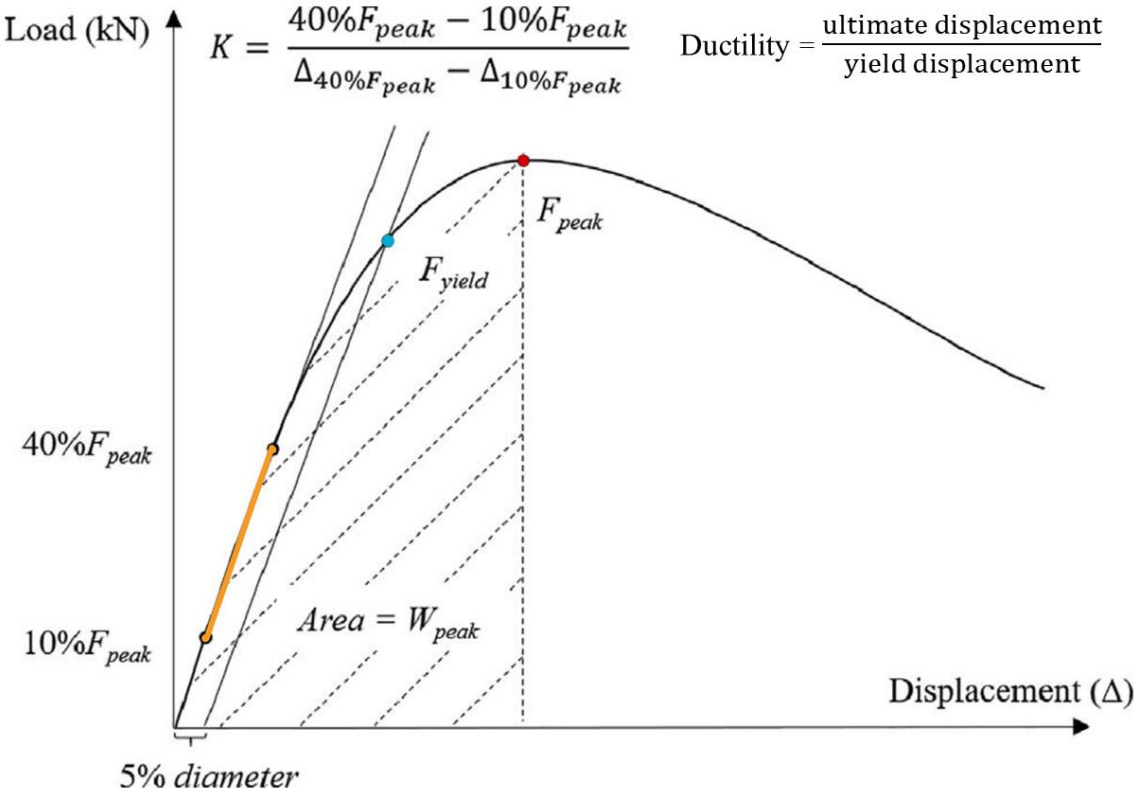

Figure 3-9 Definition of mechanical parameters (Zhu et. al., 2021).

In addition to the above mechanical properties, the specific gravity and moisture content are calculated as follows:

(1) Specific gravity:

$S_{x/y} = \frac{m_x}{V_x \rho_y}$

Where:

m_x = mass of a unit volume of a material at temperature x, g,

V_x = unit volume of a material at temperature x, cm3, and

ρ_y = density of water at temperature y, g/cm3.

(2) Moisture content:

MC, % = (A -B)/B ×100

where:

A = original mass, g, and

B = oven-dry mass, g.

4 Results and discussion

4.1 Moisture content and specific gravity

After conditioning, the moisture content and specific gravity of the substrate wood blocks and dowels were calculated and the results are given in Table 4-1. It could be found that dowels had a larger average specific gravity than S-P-F wood blocks. According to Leban and Pizzi (2007), the species used to make dowels are usually high-density hardwoods, which was confirmed in this study. The CoV results of S-P-F wood blocks are higher. This is because the wood block was cut from the various lumber pieces, resulting in a large spread of moisture content and density.

	Moisture content			Specific gravity		
	Mean (%)	S.D. (%)	CoV (%)	Mean (g/cm^3)	S.D. (g/cm^3)	CoV (%)
Wood blocks	10.98	0.06	13.4	0.44	0.08	15.8
Dowel	5.39	0.01	5.4	0.74	0.03	4.3

Table 4-1 Moisture content and specific gravity of the materials used.

4.2 Load-slip curves

The load-slip curves and average curves of each set are plotted and shown in Figures 4-1 to 4-7. It is obvious that each curve of a bolted joint specimen has four stages. At the beginning, the load increases slowly with the slip increasing quickly due to the initial 1-2mm gap between the bolt and pre-drilled hole. This is because according to the ASTM standard, the diameter of the pre-drilled hole should be 0.8 mm to 1.2mm larger than the bolt diameter when being bolted. Therefore, there exists a gap between the two contact surfaces, and the load in this slip range does not increase. Then, the load increases linearly when the load is applied. When the load exceeds the linear region, the load increases more slowly with the slip and reaches non-linear region. After the load reaches the maximum value, the joint specimen can maintain a stage of considerable bearing capacity.

As for a push-in or welded joint specimen, the load-slip curve shows three period, when the load is applied, the load increases linearly. The load exceeded the linear region and slowly increased with the slip to reach the non-linear region. After the maximum load is reached, the joint specimen can be maintained for a stage of considerable bearing capacity.

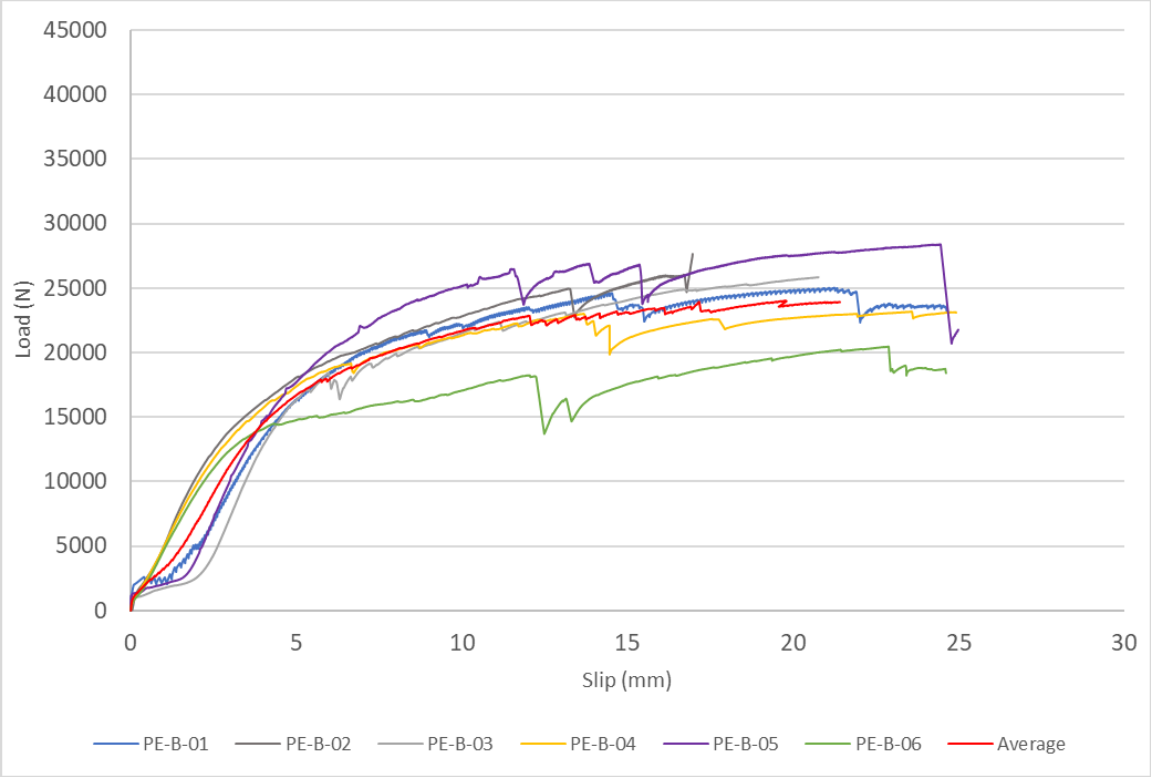

Figure 4-1 Load-slip curves of bolted joint specimens of set PE-B.

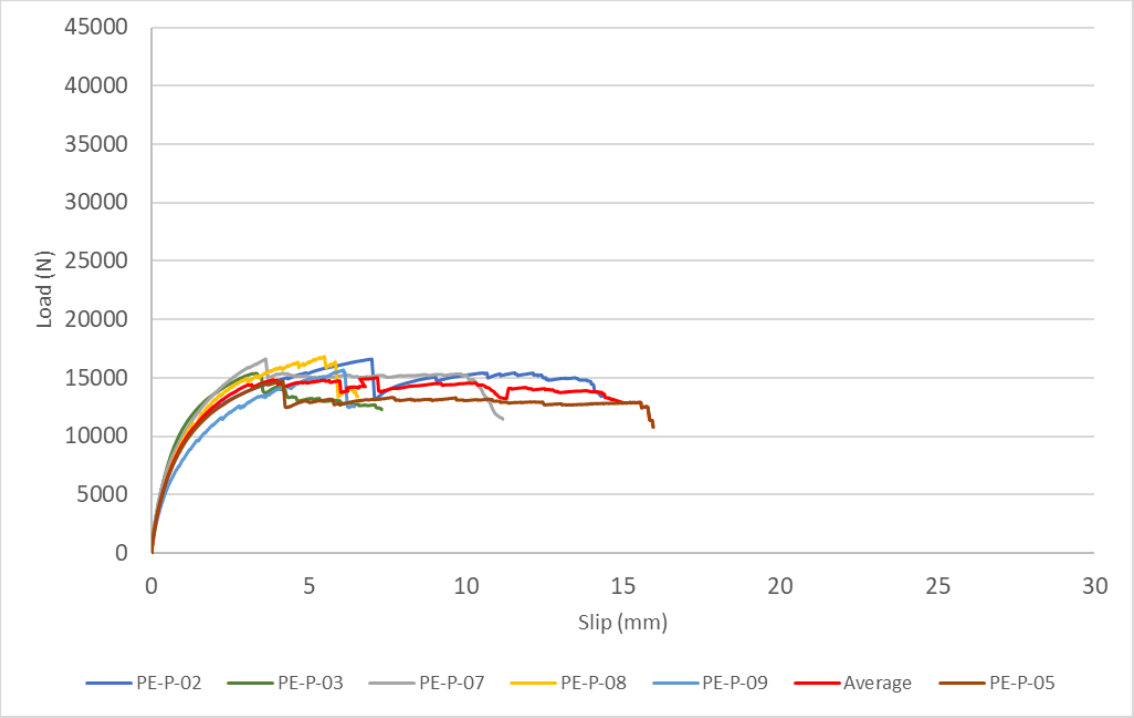

Figure 4-2. Load-slip curves of push-in joint specimen of set PE-P.

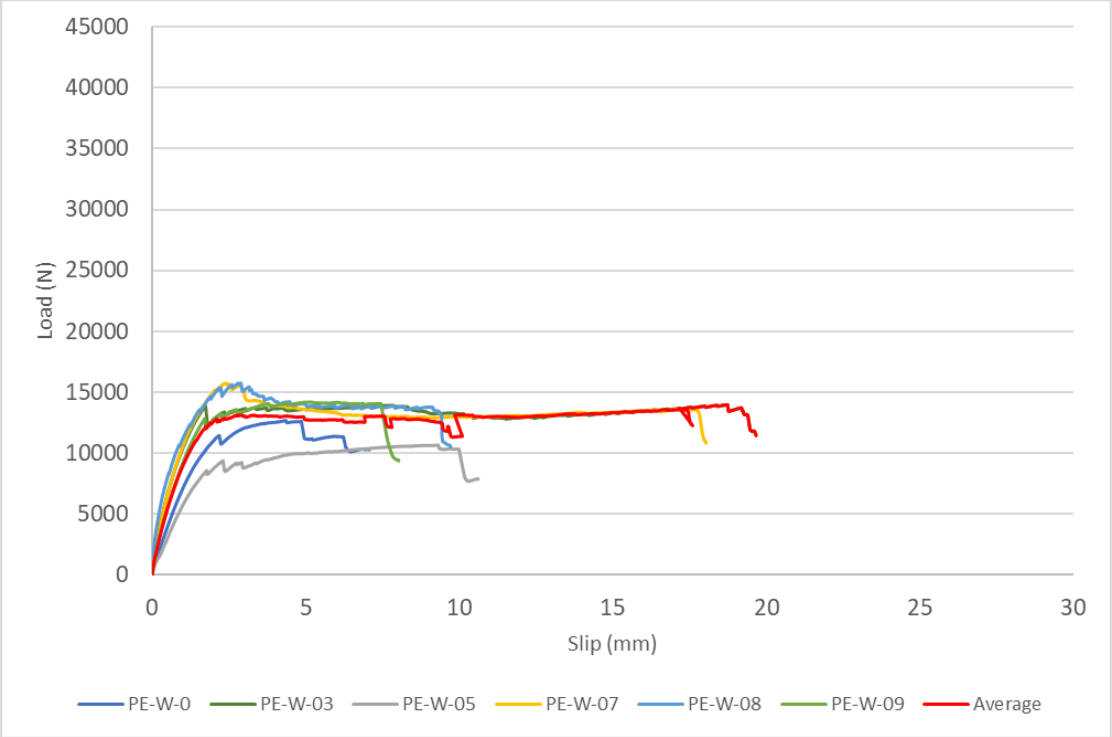

Figure 4-3 Load-slip curves of welded joint specimen of set PE-W.

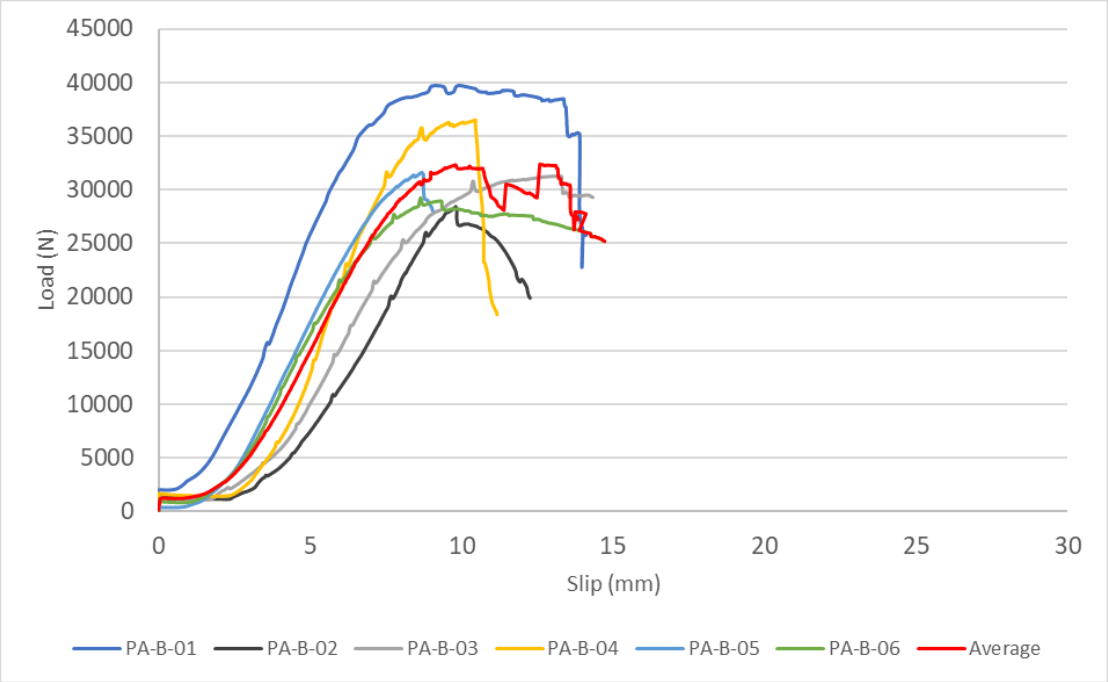

Figure 4-4 Load-slip curves of bolted joint specimen of set PA-B.

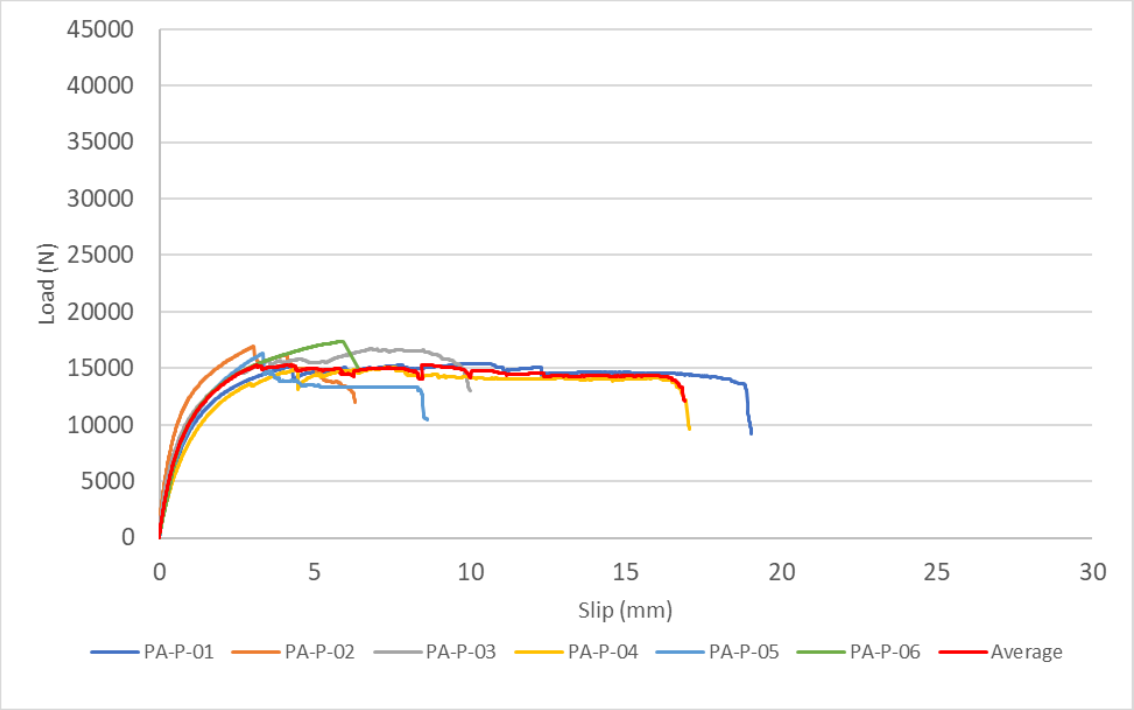

Figure 4-5 Load-slip curves of push-in joint specimen of set PA-P.

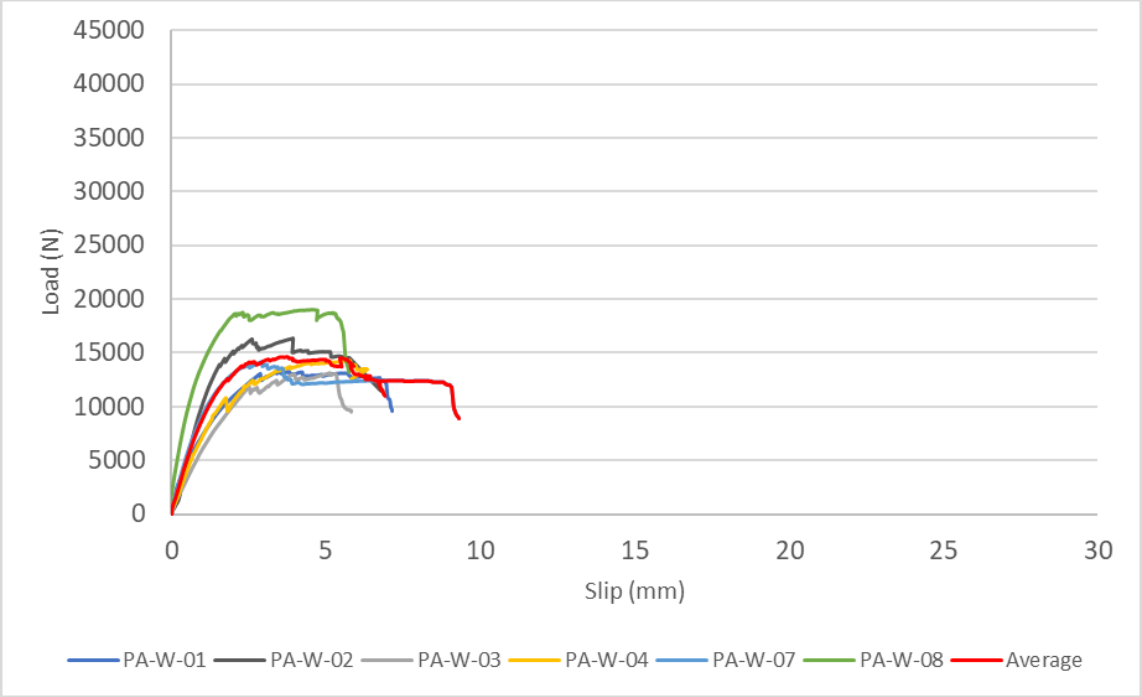

Figure 4-6 Load-slip curves of welded joint specimen of set PA-W.

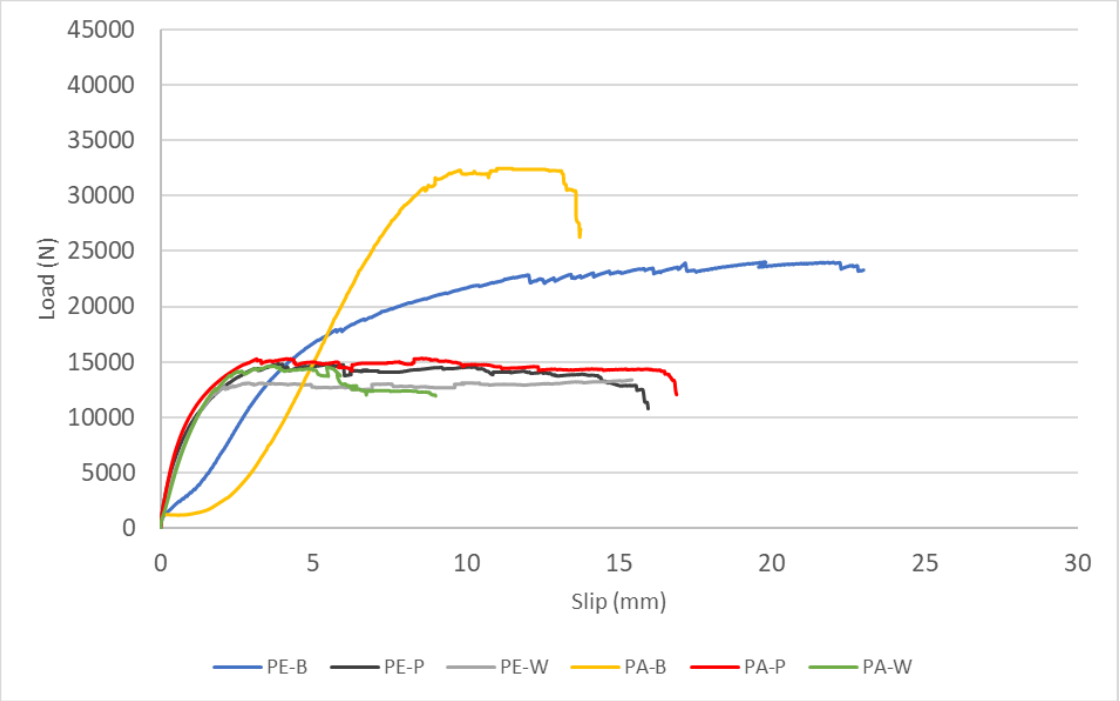

Figure 4-7 Average load-slip curves of all six sets tested in this study.

The curves of six sets in Figure 4-7 show that the sets push-in and welded show similar trends, which are independent of the loading direction, i.e., whether it is parallel or perpendicular. This was verified by the failure of wood dowels either in push-in or welded specimens, i.e., the fracture of a wood dowel under bending. In the bolted connection specimens, however, the curves exhibited are different from those of push-in and welded. Whereas the failure of bolted joint specimens is due to the damage of the wood member(s), without the failure of the bolts.

For the bolt-connected specimens, groups PA and PE curves showed a big difference. The curve of group PA shows a higher peak load value and a significant load decrease after reaching this value; for group PE curve, the sample can maintain a considerable load capacity for a longer period of time and in the non-linear region, the curve has a slight jitter. This is because when loaded perpendicular-to grain direction is similar to isotropic rubber owing to uniform properties of the lignin matrix, and a complex displacement pattern distorted by internal shear stress and slippage is produced (Samarasinghe & Kulasiri, 2000).

4.3 Failure mode

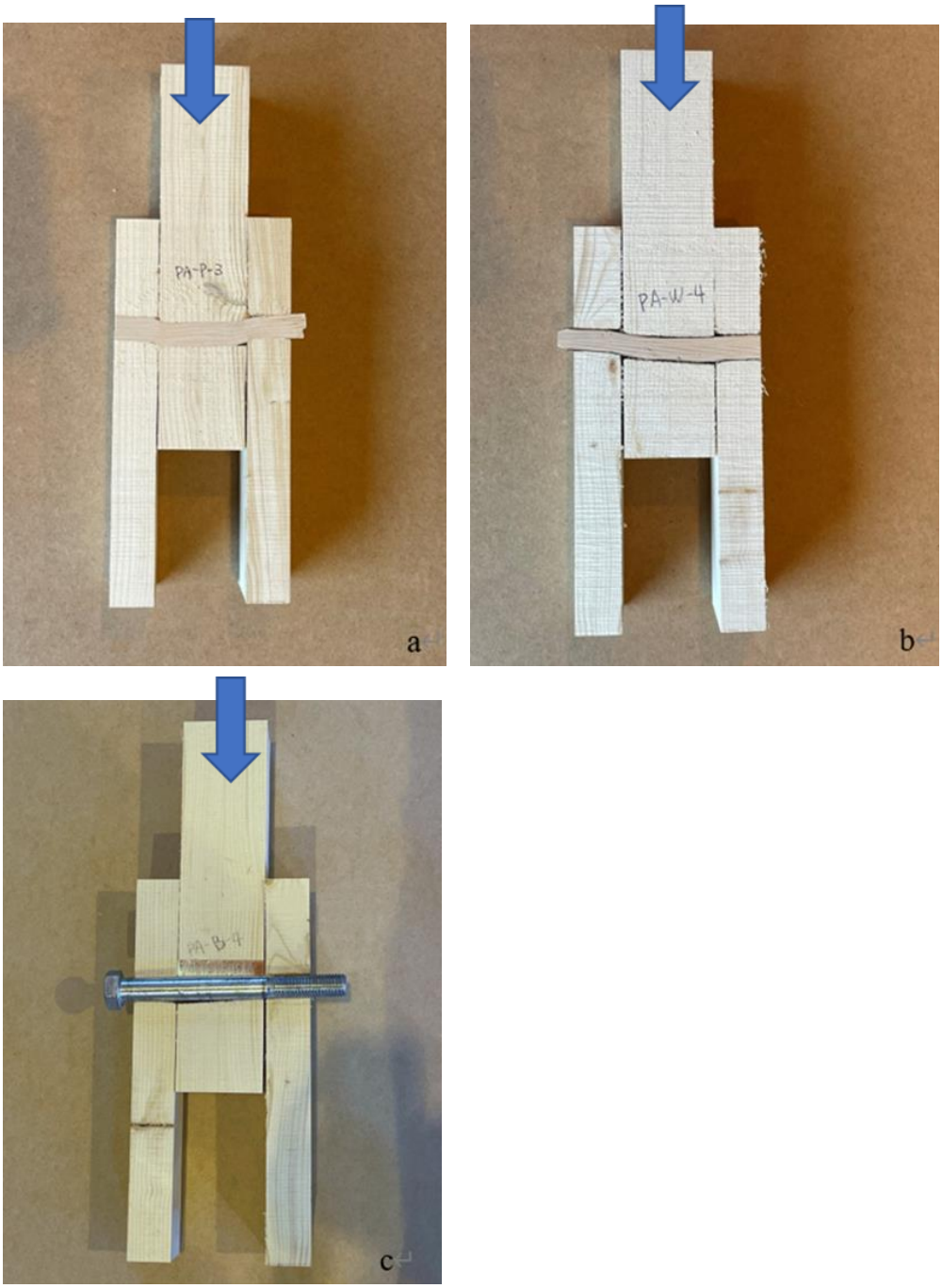

Figure 4-8 Failures of the representative joint specimens loaded in the parallel-to-grain direction after testing: (a) set push-in, (b) set welded, and (c) set bolted.

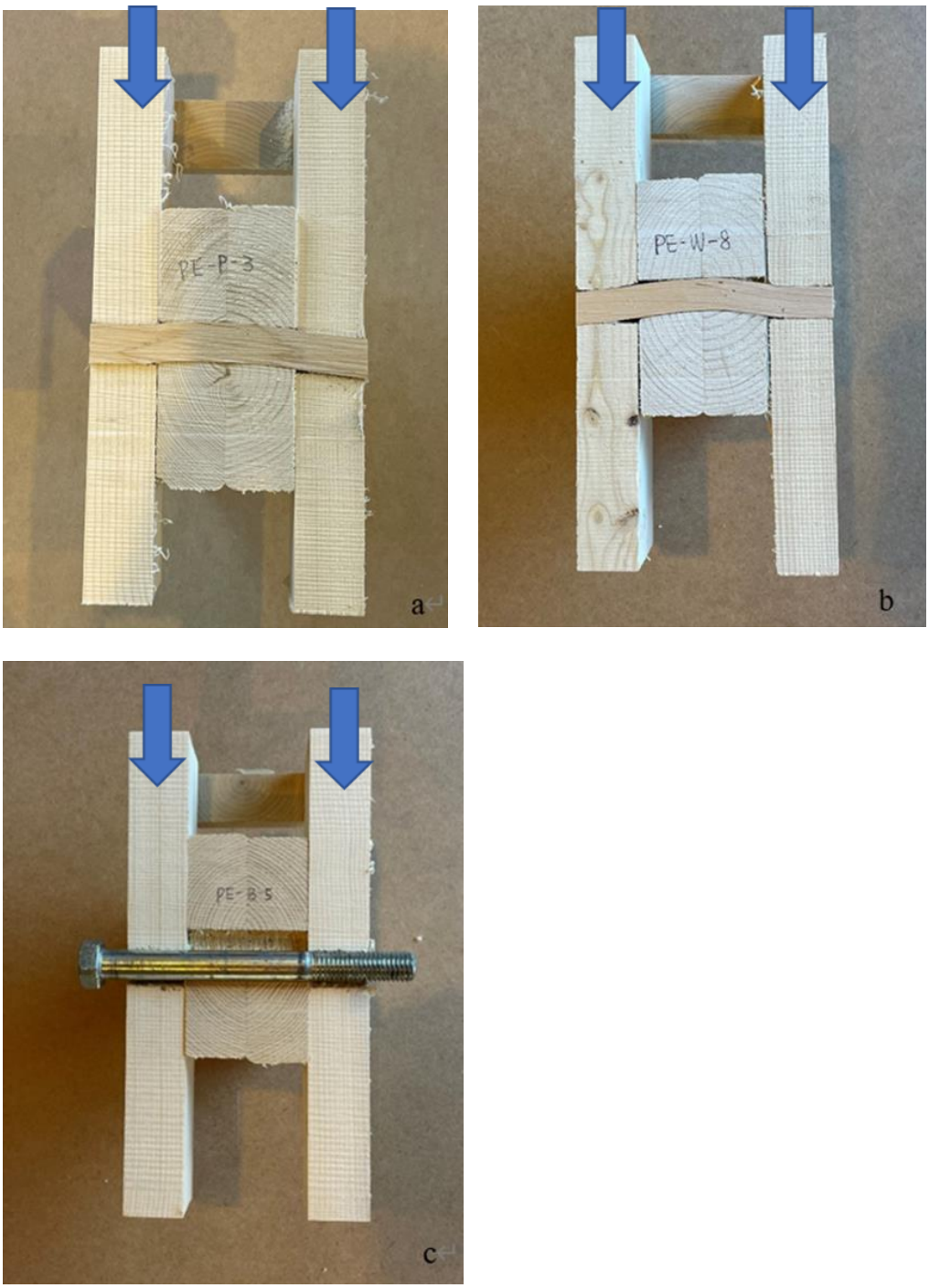

Figure 4-9 Failures of the representative joint specimens loaded in the perpendicular-to-grain direction after testing: (a) set push-in, (b) set welded, and (c) set bolted.

Figures 4-8 and 4-9 show the typical failure modes of the joint specimens tested. According to European Yield Mode of double shear 3-member joint (Johansen,1949), there are two failure modes that occur during testing, i.e., (a) the fastener does not yield but the wood deforms; and (b) the fastener yields. The type (a) occurred in the metal bolted joint sets, which can be clearly seen from Figures 4-8 and 4-9 that the metal bolts are not damaged and the central wood member was embedded and deformed along the direction of load application. However, there is a slight difference between the parallel and perpendicular bolted joint sets. The embedment happened in all three members in set PA-B, however, it mainly occurred in the central member in set PE-B. This can be attributed to the lower compressive strength of wood in the perpendicular than that in the parallel to the grain direction.

As for two dowel joint sets, the failure modes are the same, i.e., fracture of the dowel under bending. It can be found from Figures 4-8 and 4.9 that there is a slight difference in fracture mode (or deflection direction) of the dowel in terms of bending direction between parallel and perpendicular groups. For group PA, most of the fracture pattern was deformed at the central member, while for group PE, the dowels were deformed at the side members. The deformed wooden dowel occurred in the same direction as the loading direction. The load was applied on the center member for parallel specimens and on side members for perpendicular specimens.

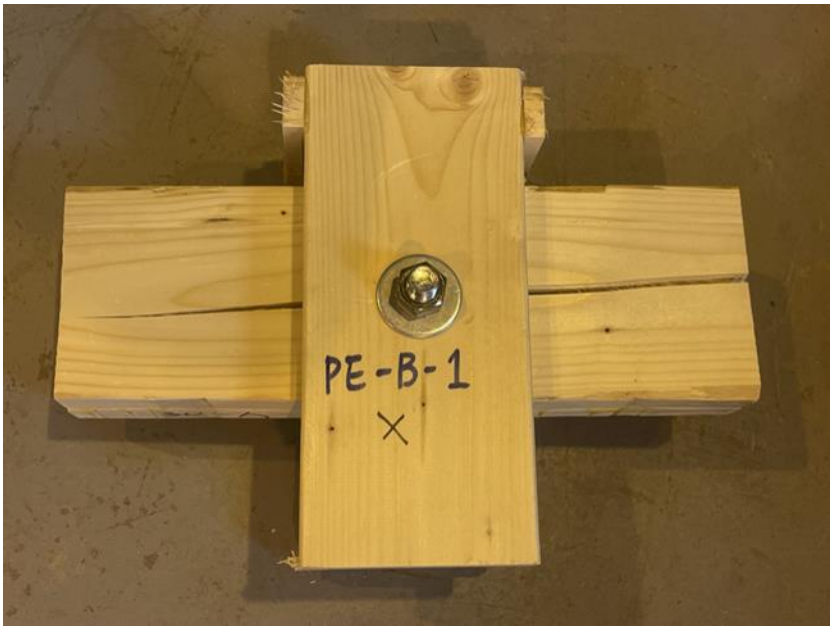

Figure 4-10 Typical failure of a bolted joint specimen loading in the perpendicular-to-grain direction.

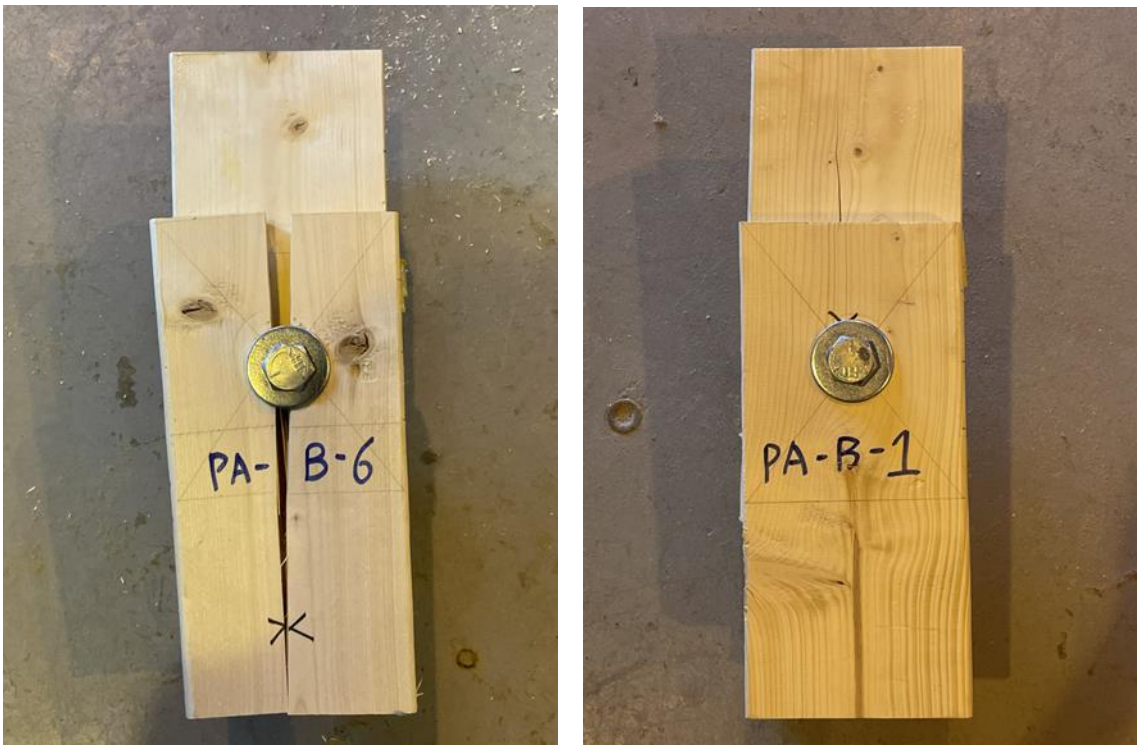

Figure 4-11 Typical failure of bolted joint specimens loaded in the parallel-to-grain direction.

Figures 4-10 and 4-11 show the failure modes of the bolted joint specimens. For group PE specimens, the fracture always happened in the central member due to the low tensile strength in the perpendicular-to-grain direction; for group PA specimens, the fracture could occur either in the side members or in the central member. It should be pointed out that all the fracture damage in a wood member was the splitting along the grain.

4.4 Mechanical properties

The peak load, initial stiffness, yield load, ductility, and energy accumulated of each specimen tested were calculated. Table 4-2 summarizes these mechanical properties of all six sets tested.

Connection type	Dowel type	Peak load (kN)			Initial stiffness (kN/mm)			Yield load (kN)			Ductility			Energy accumulated (kN·mm)		
		Mean	S.D.	CoV (%)	Mean	S.D.	CoV (%)	Mean	S. D	CoV (%)	Mean	S.D.	CoV (%)	Mean	S.D.	CoV (%)
PA	B	33	4	12	5	1	20	33	5	15	1	0	0	194	122	63
	P	16	1	6	14	4	28	13	1	7	5	2	40	80	37	46
	W	14	2	14	9	2	22	13	2	15	3	1	33	53	13	24
PE	B	24	3	12	5	1	20	11	7	63	3	1	33	292	169	58
	P	16	2	12	11	2	18	12	1	8	5	1	20	89	113	126
	W	13	2	15	11	4	36	11	3	27	4	3	75	55	67	67

Table 4-2 Means and standard deviations of mechanical properties of 6 sets tested.

4.4.1 Peak load

The average peak load values of set PA-P are 16kN and 14kN, which are 51% and 57% smaller than the value of set PA-B (33kN), respectively. This is due to the different failure modes of the members connected by bolts and wood dowels: push-in and welded specimens failed because the dowels were broken; while bolted specimens failed because the wood blocks split. Between the two dowel sets, the average peak load of set push-in was larger, which is 14% larger than that of welded dowel joint set. This is due to the loss of wood dowel material during the welding process and the destruction of the wood cells on the contact surface between the wood blocks and dowels. Group PE show similar results to those of the group PA. The average peak load values of sets push-in and welded were 33% and 45% of those of the bolted specimens. In group PE, the average peak load between sets push-in and welded have the same relationship as the parallel group, with set push-in being about 23% larger than set welded. The CoV values for sets PA-B, PA-P, and PA-W were 12%, 6%, and 14%, respectively. It can be seen that set PA-P has the lowest variation of peak load, followed by set PA-B and set PA-W. In terms of group PE, the CoV values were similar to those of group PA, but the value of set PA-P (12%) were equal to those of set PA-B.

4.4.2 Initial stiffness

The average initial stiffness values of set PA-P and set PA-W are 14 kN/mm and 9 kN/mm, which are 180% and 80% larger than that of set PA-B (of a mean initial stiffness of 5 kN/mm). This suggests that wood dowel joints have a greater initial stiffness than metal bolted ones, which is a result of the 1-2 mm gap between the bolt and pre-drilled hole in members as discussed above. Between the two dowel joint sets, the average initial stiffness of the push-in joint set was the larger, which is 55% larger than that of welded dowel joint set. This could be due to the formation of brittle char layer around the dowel in a welded dowel joint specimen, which reduces the compressive strength in both dowel and members, causing a relatively larger slip of a welded dowel joint when subjected to loading. Group PE show a similar result as group PA. The average initial stiffness of wood dowel joint specimens has a value being 120% as large as the metal bolted ones. It can be found that there is not a difference in the average initial stiffness between push-in and welded joint sets in the perpendicular direction. The CoVs of the three sets of PA-B, PA-P, PA-W were in the range of 22%-28%. The CoVs of these sets did not differ much, suggesting a high accuracy of the test results for these three sets. For group PE, the CoVs of sets PE-P and PE-W were 18% (smallest) and 36% (largest), respectively. This might be because the specimens in set PE-W were more difficult to fabricate during welding process, causing a large variation.

4.4.3 Yield load

The average yield load value is the same in sets PA-P and PA-W, that is 13kN. This is 10% smaller than the value of set PA-B. This is because for set bolted, the metal bolt does not deform, and the load is transferred directly to the wood block causing it to yield, which requires a larger force, while for sets push-in and welded, the force required for the wood dowel to yield is smaller. For group PE, the yield load values do not change much, and the values for sets bolted, push-in, and welded are 11kN, 12kN, and 11kN, respectively. The CoVs of sets PA-B, PA-P, and PA-W were 15%, 7%, and 15%, respectively. This indicated that the test results were relatively accurate among these three sets. As for group PE, it was found that the CoV of set PE-B was as high as 63%. This suggested that the results of the tests were more scattered and the reliability was low.

4.4.4 Ductility

From the perspective of the average result of ductility, the values of sets PA-P and PA-W are 5 and 3, respectively, which are 400% and 300% larger than the values of set PA-B (of a mean ductility of 1), respectively. For group PE, the values of the three sets show the same relationship as group PA, with sets PE-P and PE-W being 67% and 33% larger than that of set PE-B. However, comparing groups PA and PE, it can be found that the ductility of group PE is overall larger than those of group PA. There was a definite exponential relationship between ultimate embedment and grain angle. strength degradation (reduction in load with increasing deformation after reaching a peak load) occurs at low load-to-grain angles (Ying & Li,2001). According to the ductility calculation defined in report, because the angle of group PA was small (0 degree), it was easier for the load to reduce after reaching the peak load; that is, the displacement was smaller when reaching the specified load, so the ductility result was smaller. The CoVs of sets PA-B, PA-P, and PA-W were 0%, 40%, and 33%, respectively, indicating that the ductility results were highly variable and less reliable. The same results occurred in group PE.

4.4.5 Energy accumulation

In terms of the average energy accumulated, the results of sets PA-P and PA-W are 80kN·mm and 53kN·mm, which are 72% and 88% smaller than that of set PA-B (of a mean energy accumulated of 194kN·mm). This is due to the fact that bolted joint sets are subjected to larger loads when tested and therefore accumulate more energy. Between the two dowel joint sets, the set push-in accumulated about 51% more energy than the welded set; this is also because the specimens in push-in set are subjected to a higher load during the test. Group PE show the similar result as group PA. The energy accumulation of the dowel perpendicular joint group is approximately 69% (set push-in) and 81% (set welded) greater than that of the bolted set. The CoVs of sets PA-B, PA-P, and PA-W are 63%, 46%, and 24%, respectively. This indicated that the calculated results are discrete a lot, which is partially due to the definition and calculation of the energy accumulated. The same finding was found for group PE, where the CoVs of sets PE-B, PE-P, and PE-W were 58%, 126%, and 67%, respectively.

4.4.6 Summary

To facilitate reading, five bar charts were plotted as well showing the same contents as in Table 4-2. In general, set bolted showed better performance in terms of peak load and energy accumulation. In terms of initial stiffness and ductility, the results of sets push-in and welded were better than set bolted. Between the two dowel joint sets, the stiffness and ductility results of the push-in set were better than for the welded set. In terms of connection type, the peak load, initial stiffness, yield load, energy accumulated results are higher for group PA than for group PE. However, the ductility results of group PE are higher than those of group PA.

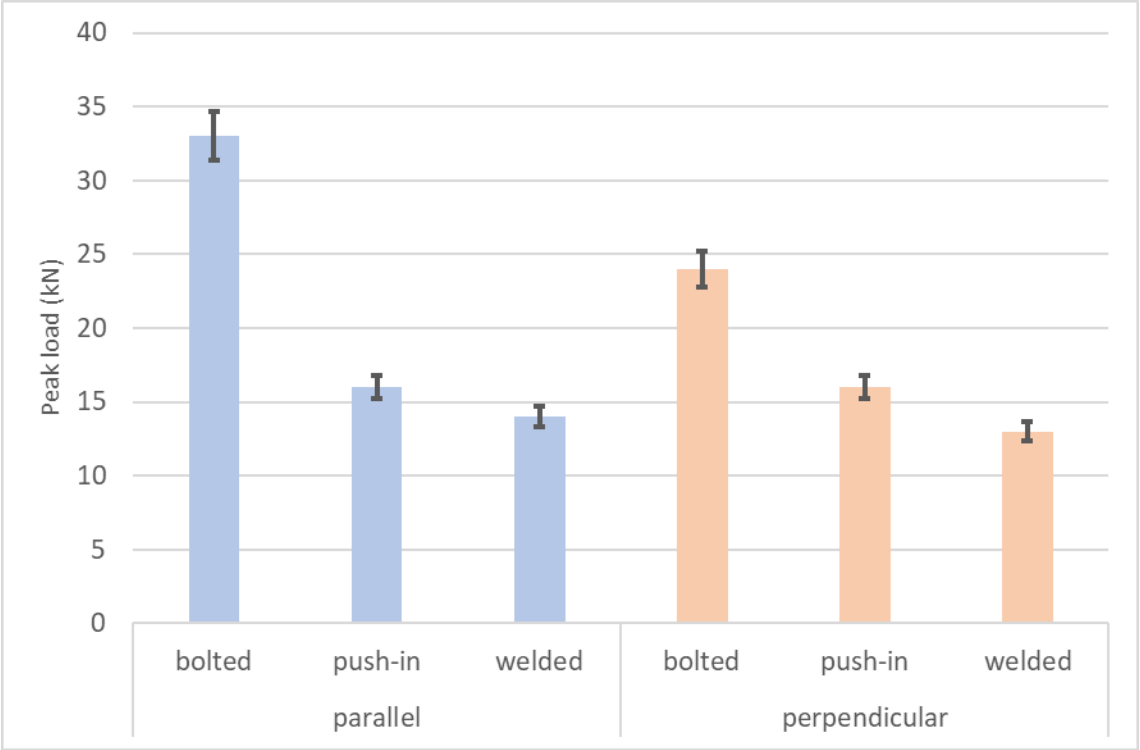

Figure 4-12 Means and standard deviations of peak load of all six joint sets tested.

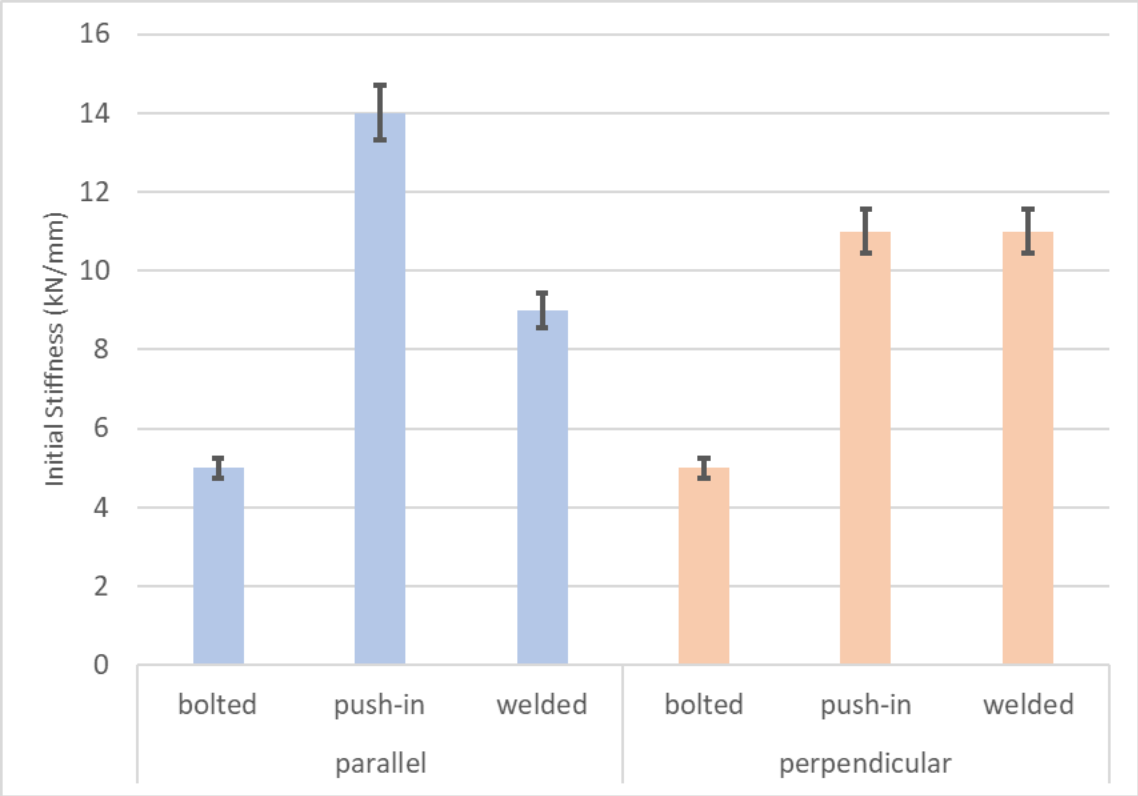

Figure 4-13 Means and standard deviations of initial stiffness of all six joint sets tested.

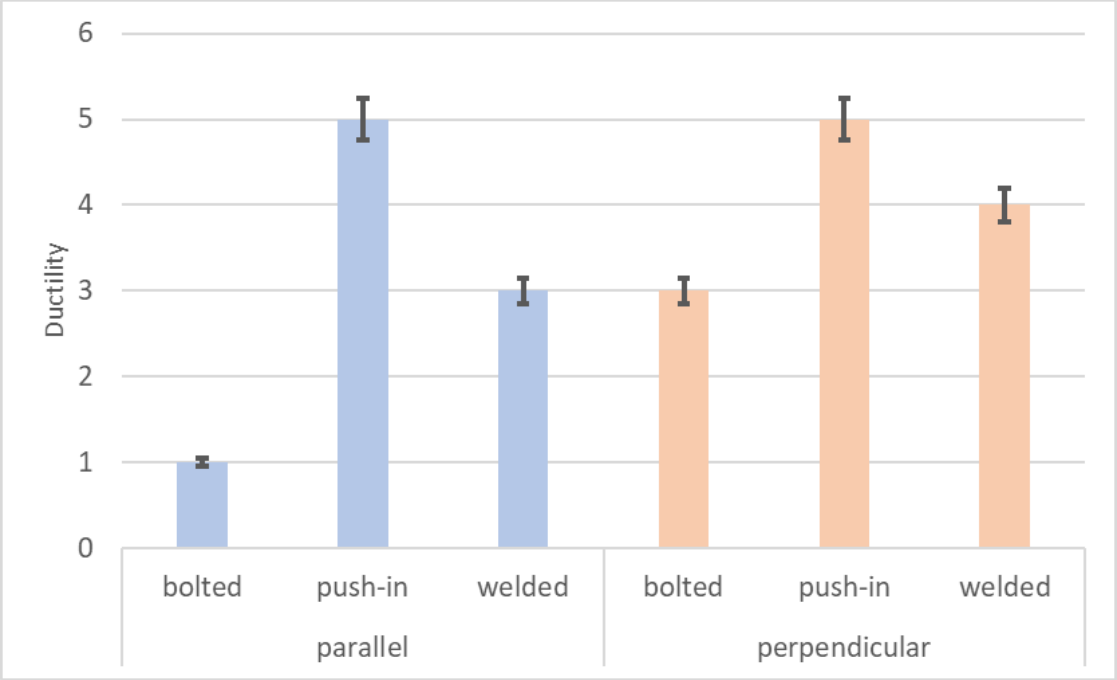

Figure 4-14 Means and standard deviations of ductility of all six joint sets tested.

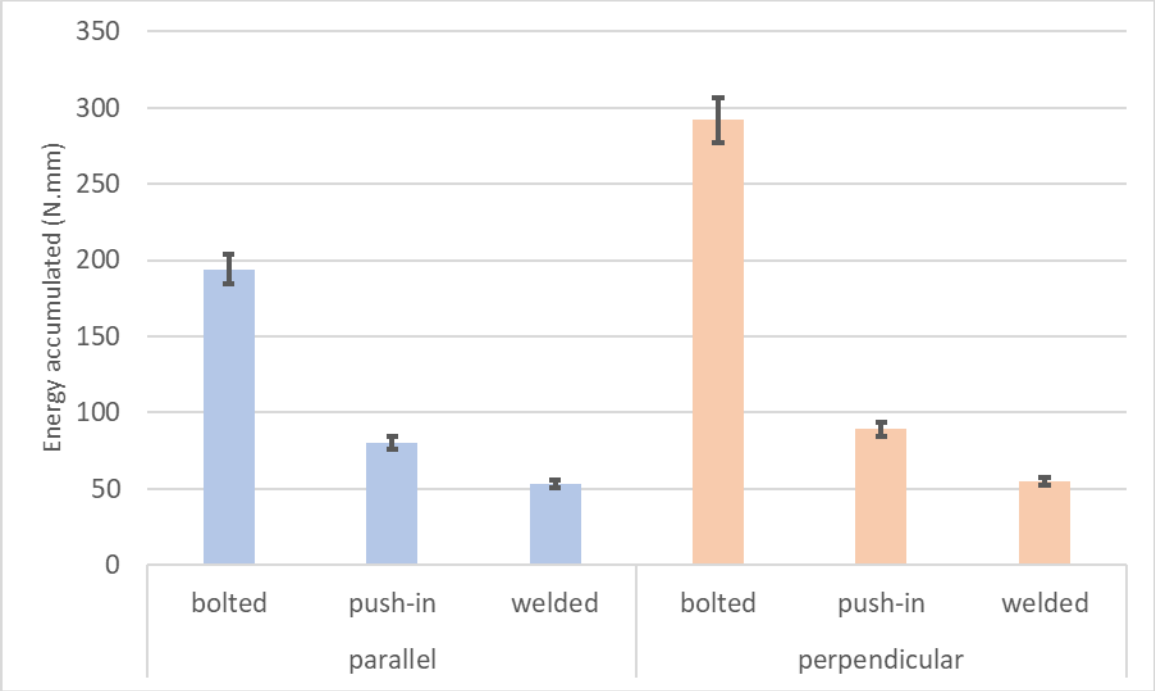

Figure 4-15 Means and standard deviations of energy accumulation of all six joint sets tested.

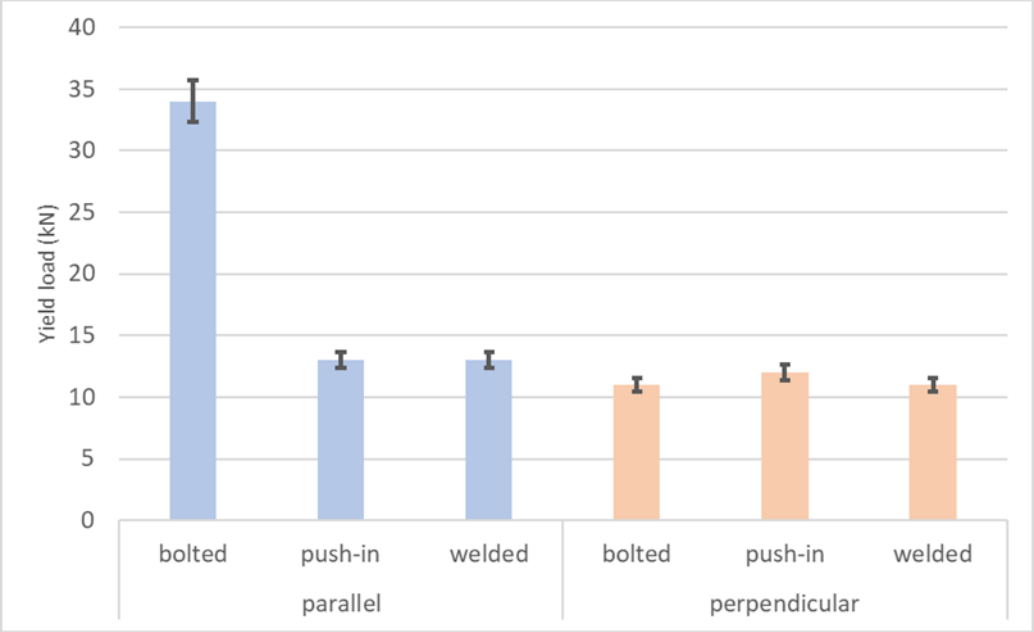

Figure 4-16 Means and standard deviations of yield load of all six joint sets tested.

On the macroscopic scale, the variability of a given mechanical property of clear wood can be mainly attributed to the grain orientation and wood density. The mechanical properties of wood decrease with an increase in the grain deviation angle (Maina & Siuda, 2020). In this study, the average densities of the substrate wood and the dowel were basically unchanged, while the grain orientation varied greatly in the connections between the parallel direction (0 degree) and perpendicular (90 degrees). Therefore, the mechanical properties of the perpendicular joint groups should be lower than those of the parallel joint ones, which was verified in this study.

During the joint test, a bolt was not deformed due to its high stiffness and strength. Thus, the load was directly transferred to the wood surface in contact with it, so the wood could be deformed in the loading direction. The interfacial friction of wood friction welding was the result of the interaction of fiber shear, winding, and high-temperature carbonization between the dowel surface and the reserved hole surface of the wood members (Gfeller & Zantti, 2018). The surface carbonization did not increase the interfacial friction force. After friction welding, the dowel forms a certain taper. The diameter of the part involved in friction decreased due to carbonization and deformation. The deformation of the part was due to the effect of welding pressure; the wood cells were subjected to pressure, and the cell walls were crushed. Thus, the dowel was soldered and showed a conical shape. However, when the diameter of the first part involved in friction decreased to a certain extent, it no longer decreased because the dowel and pre-drill hole formed a certain size fit (Yin and Zheng, 2021). Therefore, in this study, the mechanical properties of the welded joint specimens were generally lower than those of the push-in ones. This is because the

dowel causes the loss of wood materials during the welding process, in which high-speed friction caused a decrease in diameter of the dowel. Meanwhile, the wood cells on the welding contact surface were crushed and the fibers were melted, which influenced the strength of the joint specimen.

4.5 Comparison between European Yield Model and experimental curves

With the results derived from this experiment, the yield load per fastener could be predicted based on Johansen's Theory. According to CSA O86 Clause 12.4.4, the yield load of 3-member connections can be calculated for cases a), c), d), and g). The formulas are given in Figure 2-13, and given again as follows:

a) $f_1 d_F t_1$

c) $\frac{1}{2} f_2 d_F t_2$

d) $f_1 {d_F}^2 \left(\sqrt{\frac{1}{6} \frac{f_2}{(f_1+f_2)} + \frac{1}{5} \frac{t_1}{d_F}} \right)$

g) $f_1 {d_F}^2 \sqrt{\frac{2}{3} \frac{f_2}{(f_1+f_2)} \frac{f_y}{f_1}}$

where:

d_F = nominal diameter of fastener, mm

t_1, t_2 = bearing length of fastener in members 1 and 2 in accordance, mm

f_1, f_2 = embedment strength of members 1 and 2, MPa

f_y = yield strength of fastener in bending, MPa

For wood members:

$f_1 = f_2 = 50G(1\text{-}0.01d_F) \times SG = 50 \times (1\text{-}0.01 \times 19) \times 0.44 = 17.82$MPa

$n_u = f_1 d_F t_1 = 11{,}850$N (a)

$n_u = \frac{1}{2} f_2 d_F t_2 = 11{,}850$N (c)

$n_u = f_1 {d_F}^2 \left(\sqrt{\frac{1}{6} \frac{f_2}{(f_1+f_2)} + \frac{1}{5} \frac{t_1}{t_F}} \right) = 9{,}944$N (d)

$n_u = f_1 {d_F}^2 \sqrt{\frac{2}{3}\frac{f_2}{(f_1+f_2)}\frac{f_y}{f_1}}$ = 15,491N (g)

n_u is the unit lateral yielding resistance per share plane. The lowest n_u value is 10 kN, which is selected as the design value and given in Table 4-3. It can be found that except set PA-B, the predicted yield load of the most joint sets is close to those tested in this study (Table 4-3), with a deviation of about 9%-23%. The actual yield load of a joint set, except set PA-B, was higher than the predicted value. This is likely because the diameter of a dowel was relatively large during the double-shear connection test in this study. Thus, the offset displacement was also large when using the 5% diameter offset method, up to 0.95mm. Therefore, the yield strength obtained from the load-slip curve was relatively large. The finding here also suggests the value calculated using Johansen Theory is conservative and good for engineering design of wood dowelled and metal bolted joints.

Test sets	Johansen-predicted value (kN)	Experimental yield value (kN)	Failure Mechanism	Relative error (%)
PA-B	10	33	ModeI	69
PA-P		13	ModeIII	23
PA-W		13	ModeIII	23
PE-B		11	ModeI	9
PE-P		12	ModeII/III	18
PE-W		11	ModeIII	9

Table 4-3 Comparison of predicted value with experimental value.

5 Conclusions and Recommendation

This study was aimed at investigating the feasibility of applying the wood welding technique to make the wood connections for timber structural applications. To reach this objective, two factors were taken into account to examine their effects on the mechanical properties of dowel-type connections, i.e., dowel type (bolted, push-in, and welded) and loading directions, i.e., parallel and perpendicular. S-P-F lumber was used as joint members, and sugar maple dowels and metal bolts were employed as fasteners. The wood welding technique was applied to make dowelled joint specimens. Connection tests were carried out on the universal mechanical testing machine. Failure modes of each type of joint specimens were observed and recorded. The testing results were compared to the predicted values using the Johansen Theory. The main findings can be summarized as follows:

(1) The average peak load and initial stiffness of set PA-B were 33kN and 5kN/mm, which were about 135% larger than and 45% less than set PA-W (14kN and 9kN/mm). Within the two wood dowel sets, the average peak load and initial stiffness of set PA-P were 16kN and 14kN/mm, which were 14% and 50% larger than that of set PA-W.

(2) Within the two wood dowel sets, the average yield loads of sets PA-P and PA-W were about the same, being 13kN. The average yield load of set PA-B was 33kN, which was 150% larger than that of set PA-P or set PA-W.

(3) The average ductility and energy accumulated of set PA-B were 1 and 194kNmm, which were about 30% less than and 160% larger than sets PA-P and PA-W.

(4) In terms of connection types, the average peak load and initial stiffness of group PA were about 25% and 27% greater than those of group PE.

(5) Johansen Theory was conservative to derive the engineering design values for the wood dowelled and metal bolted joints.

(6) The failure of wood doweled joint specimens was the fracture of the dowels, and the failure of bolted joint specimens was the crushing of member wood.

(7) The mechanical properties of welded joints were similar to those of push-in joints.

(8) The welding process did not generate cracks, minimizing stress concentrations, in wood members, in comparison to push-in process. It has great potential in fabrication of dowel-laminated wood products and repair/reinforcement of laminated beams.

The next step should be to optimize the experimental parameters and processing procedures to determine the best process conditions. Furthermore, application of welding techniques should be explored during the manufacturing and construction of timber products and buildings, such as reinforcing glued laminated wood with notches.

References

Auchet. S., Segovia. C., and Mansouri. H.R. (2010). Accelerating vs constant rate of insertion in wood dowel welding. [J] *Journal of adhesion science and technology*, 24:7, 1319-1328.

Belleville, B., Pizzi, A., and Segovia, C. (2012). Wood Blockboards Fabricated by Rotational Dowel Welding. [J]. *Journal of Adhesion Science and Technology, 25*(2011):2745-2753.

Belleville, B., Stenvanovic, T., and Pizzi, A. (2012). Determination of optimal wood-dowel welding parameters for two North America hardwood species. [J]. *Journal of Adhesion Science and Technology,* 27:5-6, 556-576.

Bocquet, J., Pizzi, A., and Despres, A. (2007). Wood joints and laminated wood beams assembled by mechanically-welded wood dowels. [J]. *Journal of Adhesion Science and Technology,* 21:3-4, 301-317.

Boonstra, M., and Pizzi, A. (2006). Vibration welding of heat-treated wood. [J] *Journal of Adhesion Science and Technology*, 20:4, 359-369.

Bocquet, J., Pizzi, L. (2012). Full-scale (industrial) wood floor using welded-through dowels. [J]. *Journal of Adhesion Science and Technology*, 20:15, 1727-1739.

Cornault, P.R., and Carpentier, L. (2020). Tribological mechanisms involved in Friction wood welding. [J]. *Tribology International 141*(2020), 105963.

Ebner, M., and Petutschnigg, A. (2014) Development of an automated wood welding process. [J] *Journal of Adhesion Science and Technology*, 28:18, 1783-1791.

Forest Products Laboratory (U.S.). (1974). *Wood handbook: wood as an engineering material* (Revised, Ser. Agriculture handbook, no. 72). Laboratory.

Gfeller, B., and Zanetti, M. (2003). Wood bonding by vibrational welding. [J]. *Journal of Adhesion Science and Technology,* 17:11,1573-1589.

Ganne, C., and Pizzi, A. (2005) Parameter interactions in two-block welding and the wood nail concept in wood dowel welding. [J]. *Journal of adhesion science and technology*, 19:13-14,1157-1174.

Ganne, C. (2005). Temperature and density distribution in mechanical vibration wood welding. [J]. *Wood Science Technology* (2006), 40:72-76.

Ganne, C., Pizzi, A., and Thomas, A. (2005). Parameter interactions in two-block welding and the wood nail concept in wood dowel welding. [J]. *Journal of Adhesion Science and Technology,* 19:13-14, 1157-1174.

Girardon, S., Barthram, C., and Resch, L. (2014). Determination of shearing stiffness parameters to design multi-layer spruce beams using welding-through wood dowels. [J]. *Eur. J. Wood Prod.* (2014) 72:721–733.

Johansen, K. W. (1949). Theory of timber connections. [J]. *Int Assoc Bridge and Struct Eng*, 9: 249-262.

Johansson, H., & Stehn, L. (2002). Ductility aspects in nailed glue laminated timber connection design. [J]. *Journal of Structural Engineering*, 128(3), 382–389.

Kanazawa, F., and Pizzi, A. (2005) Parameter influencing wood-dowel welding by high-speed rotation. [J] *Journal of adhesion science and technology*,19:12, 1025-1038.

Leban, M., Pizzi, A. and Porperzi, M. (2007). Wood welding: A challenging alternative to conventional wood gluing. [J]. *Scandinavian Journal of Forest Research*, 20:6,534-538.

Li, Y., and Chui, Y.H. (2001). Empirical Models Depicting Grain Angle Effects on Load-

Embedment Response of Dowel-Type Fasteners in Wood. [J]. ASTM Int'l.

Mania, P., Siuda, F., & Roszyk, E. (2020). Effect of slope grain on mechanical properties of different wood species. *Materials* (Basel, Switzerland), 13(7).

Mansouri, H., Pizzi, A., and Leban, J.M. (2012). Causes for the Improved Water Resistance in Pine Wood Linear Welded Joints. [J]. *Journal of Adhesion Science and Technology,* 25:16, 1987-1995.

Murty, B., Asiz, A., & Smith, I. (2011). Tests and models for engineered wood product connections using small steel tube fasteners. [J].*Engineering Structures*, 33(1), 63–68.

Omrani, P., Mansouri, H.R. and Pizzi, A. (2009). Influence of Wood Grain Direction on Linear Welding. [J]. *Journal of Adhesion Science and Technology 23*(2009):2047-2055.

Omrani, P., Masson, E., and Pizzi, A. (2012). Emission Gases in Linear Vibration Welding of Wood. [J]. *Journal of Adhesion Science and Technology,* 23:1, 85-94.

Omrani, P., Masson, E., and Pizzi, A. (2008). Emission of gases and degradation volatiles from polymeric wood constituents in friction welding of wood dowels. [J]. *Polymer Degradation and Stability* 93 (2008) 794-799.

Omrani, P., Mansouri, H.R., and Duchanois, G. (2009). Fracture Mechanics of Linearly Welded Wood Joints: Effect of Wood Species and Grain Orientation. [J]. *Journal of Adhesion Science and Technology,* 23:16, 2057-2072.

Oudjene, M., Khelifa, M., and Segovia, C. (2012). Application of Numerical Modelling to Dowel-Welded Wood Joints. [J]. Journal of Adhesion Science and Technology, 24:2, 359-370.

Pizzi, A., and Mansouri, H.R. (2010). Enhancing the Exterior Performance of Wood Jointed by Linear and Rotational Welding. [J]. *Journal of Adhesion Science and Technology*

25(2011):2717-2730.

Porteous, J., and Kermani, A. (2013). Structural timber design to Eurocode 5 (2nd ed.). Wiley-Blackwell. Retrieved 2022.

Pu, X. (2020). Optimization of Machining Parameters of Rotational Welding Technology. FE Thesis Report, the University of New Brunswick, Fredericton, NB, Canada.

Rodriguez, G., Diouf, P., and Blanchet, P. (2010). Wood-Dowel Bonding by High-Speed Rotation Welding — Application to Two Canadian Hardwood Species. [J]. *Journal of Adhesion Science and Technology,* 24:8-10, 1423-1436.

Sawata, K. (2015). Strength of bolted timber joints subjected to lateral force.[J]. *Journal of Wood Science: Official Journal of the Japan Wood Research Society*, 61(3), 221–229.

Samarasinghe, S., and Kulasiri, G. D. (2000). Displacement fields of wood in tension based on image processing: part 1. Tension parallel- and perpendicular-to grain and comparisons with isotropic behaviour. Silva Fennica, 34, 251–259.

Segovia, C., Zhou, X., and Pizzi, A. (2012). Wood blockboards for construction fabricated by wood welding with pre-oiled dowels. [J]. *Journal of Adhesion Science and Technology,* 25:20, 2745-2753.

Segovia, C., and Pizzi, A. (2009). Performance of Dowel-Welded Wood Furniture Linear Joints. [J]. *Journal of Adhesion Science and Technology,* 23:9,1293-1301.

Stamm, B., and Natter, J. (2005) Joining wood by friction welding. [J]. *Holz als Roh-und Werkstoff*, 2005, 63(5):313-320.

Smith, I., Foliente, G., Nguyen, M., & Syme, M. (2005). Capacities of dowel-type fastener joints in 113ustralian pine. Journal of Materials in Civil Engineering, 17(6),

664.

Sun, Y., and Royer, M. (2012). Chemical Changes Induced by High-Speed Rotation Welding of Wood — Application to Two Canadian Hardwood Species. [J]. *Journal of Adhesion Science and Technology,* 24:8-10, 1383-1400.

Tondi, G., and Andrews, S. (2007) Comparative potential of alternative wood welding systems, ultrasonic and micro friction stir welding. [J]. *Journal of Adhesion Science and Technology*, 21:16, 1633-1643.

Vaziri, M., Karlsson, O., and Abrahamsson, L. (2020). Wettability of welded wood-joints investigated by the Wilhelmy method. [J]. *Holzforschung* 2021, 75(1):79-86.

Wilkinson, T. L. (1993). Bolted connection design values based on European yield model. [J]. *Journal of Structural Engineering*, 119(7), 2169–2186.

Yin, W., Zheng, Y., Lu, H., and Tian, Y. (2021). Tribological and mechanical properties of wood dowel rotation welding with different additives. [J]. *Journal of Adhesion Science Technology*, Dec2021, P1.

Zoulalian, A., and Pizzi, A. (2006). Wood-dowel rotation welding—a heat-transfer model. [J]. *Journal of Adhesion Science and Technology,* 21:2, 97-108.

Zhang, J., and Gao, Y. (2018). Influence of pretreated wood dowel with $CuCl_2$ on temperature distribution of wood dowel rotation welding. [J]. *Journal of Wood Science,* 64:209-219.

Zhu, X., and Gao, Y. (2017). Mechanics and pyrolysis analyses of rotation welding with pretreated wood dowels. [J]. *Journal of Wood Science,* 63:216-224.

Zhu, W., and Gong, M. (2021). Improved fastening designs for bridge decks made of mechanically laminated timber. [J]. *Construction and Building Materials*, 266 (2021).

Curriculum Vitae

Candidate's full name: Xiaoyu Wang

Universities attended:

Nanjing Forestry University, Bachelor of Science in Engineering (Wood Science and Engineering), P.R. China, 2021

University of New Brunswick, Exchanging Student (2020-2021)

University of New Brunswick, Master of Forestry Engineering, 2022